Universidade de Aveiro Departamento de Biologia
Ano 2013/2014

Marcos Levi dos Santos Cardoso

HIF-1α RELEVANCE IN NECROSIS OF *MYCOBACTERIUM AVIUM*-INDUCED GRANULOMAS

RELEVÂNCIA DO HIF-1α NO GRANULOMA MICOBACTERIANO

Universidade de Aveiro Departamento de Biologia
Ano 2013/2014

Marcos Levi dos Santos Cardoso

HIF-1α RELEVANCE IN NECROSIS OF *MYCOBACTERIUM AVIUM*-INDUCED GRANULOMAS

RELEVÂNCIA DO HIF-1α NO GRANULOMA MICOBACTERIANO

Dissertação apresentada à Universidade de Aveiro para cumprimento dos requisitos necessários à obtenção do grau de Mestre em Biologia Molecular e Celular, realizada sob a orientação científica da Doutora Margarida Maria Coutinho Nogueira Marta Borges, Professora Auxiliar do Departamento de Ciências Biológicas da Faculdade de Farmácia da Universidade do Porto e Doutora Maria de Fátima Matos Almeida Henriques de Macedo, Professora Auxiliar Convidada da Secção Autónoma de Ciências da Saúde da Universidade de Aveiro.

“As you set out for Ithaka
hope the voyage is a long one,
full of adventure, full of discovery.
Laistrygonians and Cyclops,
angry Poseidon—don’t be afraid of them:
you’ll never find things like that on your way
as long as you keep your thoughts raised high,
as long as a rare excitement
stirs your spirit and your body.

Hope the voyage is a long one.
May there be many a summer morning when,
with what pleasure, what joy,
you come into harbors seen for the first time;
may you stop at Phoenician trading stations
to buy fine things,
and may you visit many Egyptian cities
to gather stores of knowledge from their scholars.

Keep Ithaka always in your mind.
Arriving there is what you are destined for.
But do not hurry the journey at all.
Better if it lasts for years,
so you are old by the time you reach the island,
wealthy with all you have gained on the way,
not expecting Ithaka to make you rich.

Ithaka gave you the marvelous journey.
Without her you would not have set out.
She has nothing left to give you now.

And if you find her poor, Ithaka won’t have fooled you.
Wise as you will have become, so full of experience,
you will have understood by then what these Ithakas mean”

“*Ithaka*” by Constantine P. Cavafy

o júri

Presidente

Professora Doutora Maria de Lourdes Gomes Pereira
Professora Associada com agregação ao Departamento de Biologia da Universidade de Aveiro

Professora Doutora Margarida Maria Coutinho Nogueira Marta Borges
Professora Auxiliar do Departamento de Ciências Biológicas da Faculdade de Farmácia da Universidade do Porto

Professora Doutora Maria Alice dos Santos Silva Gomes Martins
Professora Associada do Departamento de Ciências Biológicas da Faculdade de Farmácia da Universidade do Porto

Alguns dos resultados deste trabalho estão incluídos:

Artigos em revista de circulação internacional com arbitragem científica:

Cardoso MS, Silva T, Martins E, Resende M, Appelberg R, Borges M. **Lack of the transcription factor hypoxia-inducible factor (HIF)-1α in macrophages accelerates the necrosis of *Mycobacterium avium*-induced granulomas.**
Manuscrit

Resumos em revista de circulação internacional com arbitragem científica:

M. Cardoso, T. Silva, R. Appelberg, M. Borges. **Transcription factor hypoxia-inducible factor (HIF)-1alpha is relevant for necrosis of Mycobacterium avium-induced granulomas.** The FEBS Journal 281 (Suppl. 1) (2014) 65–783.

Comunicação em painel:

Cardoso MS, Silva T, Resende M, Appelberg R, Borges M.
Lack of the transcription factor hypoxia-inducible factor (HIF)-1α accelerates the necrosis of *Mycobacterium avium*-induced granulomas.
Sociedade Portuguesa de Imunologia, Lisboa, Portugal, Outubro 2014.

Cardoso MS, Silva T, Appelberg R, Borges M.
Dertermination of HIF-1α relevance in the immunopathology associated with *Mycobacterium avium* infection
FEBS-EMBO 2014 conference, Paris, França, Setembro 2014.

Comunicação oral:

Cardoso MS, Appelberg R, Borges M.
Dertermination of HIF-1α relevance in the immunopathology associated with *Mycobacterium avium* infection
IJUP'14, Porto, Portugal, Fevereiro 2014.

Agradecimentos

Durante estes dois anos há inevitavelmente muito que agradecer. Seria impossível a conclusão desta etapa se não tivesse o apoio, dedicação, entusiasmo e compreensão daqueles que me rodeiam.

Quero agradecer profundamente à Dr.ª Margarida Borges por me ter recebido como seu aluno, pela partilha de conhecimentos e experiências que me deu a oportunidade de vivenciar. Poucas palavras expressam a minha gratidão por desde o primeiro dia ter confiado, incentivado e impelido a fazer mais e melhor.

Quero também agradecer à Dr.ª Fátima Macedo por ter aceite continuar a fazer parte deste meu percurso na ciência. Se hoje estou aqui é devido ao seu entusiasmo que me transmitiu durante as suas aulas na licenciatura.

Quero também agradecer de uma forma especial ao Prof. Rui Appelberg por me ter aceite no seu laboratório e por me ter dado o prazer de apresentar o trabalho do grupo no congresso em Paris!

À Mariana e à Tânia, por estarem sempre prontas a ajudar e por terem sempre uma palavra de conforto quando as coisas não resultavam tão bem. Obrigado por tornarem o ambiente deste laboratório simplesmente fantástico!

Sinto-me sortudo porque neste percurso conheci amigos que jamais deixaram de me apoiar, mesmo que o apoio significasse ir jantar ao Mcdonald's durante as longas noites de experiências. Obrigado por todas as discussões pseudo-científicas, por todos os lanches e momentos inesquecíveis! Foi um prazer aturar-vos durante estes dois anos! Obrigado Ana, Rita e Sandra!

Ao OD Team, aos runners, aos Desbravadores, amigos de infância e a família maravilhosa! Obrigado por cada jogo de futebol, por cada corrida, por cada acampamento, por cada momento à volta de uma mesa e por cada palavra! Obrigado por me ajudarem a lembrar que há vida além da tese!

Às minhas little girls por todo o apoio, preocupação constante e por contribuírem de uma forma tão extraordinária naquilo que sou hoje. Sou um sortudo em ser o vosso irmão mais velho!

Aos heróis da minha vida! Jamais chegaria aqui sem vocês! Por cada almoço, por cada palavra, por cada ato, por tudo o que fizeram, fazem e irão continuar a fazer por mim.

palavras-chave Necrose; HIF-1α; *Mycobacterium avium*; Granuloma; Hipoxia.

Resumo

O desenvolvimento da infeção por micobactérias é caracterizado pela formação de granulomas, os quais são agregados bem organizados de células do sistema imunitário, nomeadamente macrófagos infetados. A principal função do granuloma é restringir e prevenir a disseminação da micobactéria permitindo que a resposta imunitária seja centrada numa área limitada. Por vezes, estas lesões aumentam em tamanho, progredindo para um processo de necrose central levando à caseação tecidular. Contudo, o mecanismo subjacente a este tipo de patologia é pouco compreendido. Tem sido descrito que a redução da vascularização dos granulomas é essencial para a sua caseação e alguns estudos demonstraram que o centro do granuloma é altamente hipóxico. Em condições de hipóxia as células do sistema imunitário necessitam de se adaptar rapidamente a concentrações de oxigénio baixas de forma a permanecerem funcionalmente ativas. Assim, o fator indutível por hipóxia – 1 alfa (HIF-1α) tem emergido como o principal regulador do sistema de adaptação à hipoxia, mediando uma série de mecanismos fisiológicos e celulares. O grupo de investigação da responsabilidade do Professor Appelberg, desenvolveu um modelo de estudo que mimetiza a necrose do granuloma observado durante a infeção por *Mycobacterium tuberculosis* em humanos. Este modelo consiste na infeção intravenosa de murganhos C57BL/6 com uma dose baixa de uma estirpe altamente virulenta de *Mycobacterium avium* (ATCC 25291). Estes murganhos desenvolvem granulomas necrosados após 4 meses de infeção. Para determinar a relevância do HIF-1α durante a infeção por *M. avium*, foram utilizados murganhos com células da linhagem mielóide deletadas para o fator HIF-1α sobre o controlo do sistema Cre-lox. Os resultados obtidos indicam que os murganhos deficientes em HIF-1α são mais suscetíveis à infeção e em que o aparecimento de granulomas necróticos é antecipado.

Keywords Necrosis; HIF-1α; *Mycobacterium avium*; Granuloma; Hypoxia.

Abstract

The establishment of mycobacterial infection is characterized by the formation of granulomas, which are well-organized aggregates of immune cells, namely infected macrophages. The granuloma main function is to constrain and prevent dissemination of the mycobacteria, while concentrating the immune response to a limited area. In some cases these lesions can grow progressively into large granulomas which can undergo central necrosis leading to their caseation. However, the mechanism underlying this type of pathology is still poorly understood. It has been reported that reduced vascularization of granulomas may be one essential mechanism for caseation and some studies have demonstrated severely hypoxic regions at the center of the granuloma. Under hypoxic conditions the immune cells need to adapt to low oxygen conditions in order to remain functionally active. Thus, the hypoxia-inducible factor – 1 alpha (HIF-1α) has emerged as a master regulator of the hypoxia adaptation system, mediating a wide range of physiological and cellular mechanisms. The Appelberg group has developed a granuloma necrosis model that mimics the human pathology of *Mycobacterium tuberculosis*, using C57BL/6 mice intravenously infected with a low dose of a highly virulent strain of *Mycobacterium avium* (ATCC 25291). Such mice develop granulomas that, at 4 months of infection, exhibit central necrosis. To determine the relevance of HIF-1α during *M. avium* infection we used a mouse strain deleted of HIF-1α under the Cre-lox system in the myeloid cell lineage. The results obtained indicate that HIF-1α deficient mice are more susceptible to the infection and that the onset of necrotic granulomas is faster.

Contents

Figures

ABBREVIATIONS

AIDS	Acquired immune deficiency syndrome
APC	Antigen presenting cells
ATCC	American type culture collection
ATP	Adenosine triphosphate
CD	Cluster of differentiation
CFU	Colony-forming unit
DC	Dendritic cell
ELISA	Enzyme-linked immunosorbent assay
HIF-1α	Hypoxia-inducible factor-1 alpha
HIV	Human immunodeficiency virus
HRE	Hypoxia-response elements
IFN-γ	Interferon gamma
Ig	Immunoglobulin
IL	Interleukin
iNOS	Inducible nitric oxide synthase
LPS	Lipopolysaccharide
MAC	*Mycobacterium avium* complex
M. avium	*Mycobacterium avium*
mRNA	Messenger ribonucleic acid
MHC	Major histocompatibility complex
M. tuberculosis	*Mycobacterium tuberculosis*
MyD88	Myeloid differentiation factor 88
NF-κB	Nuclear factor- kappa B
NK	Natural killer
NKT	Natural killer T cell
Nramp1	Natural resistance associated macrophage protein 1
NTM	Nontuberculosis mycobacteria

NO	Nitric oxide
0_2	Oxygen
PET	Positron emission tomography
PRR	Pattern recognition receptor
Pvhl	Von Hippel-Lindau tumor suppressor protein
ROS	Reactive oxygen species
Slc11a1	Solute carrier family 11a member 1
TB	Tuberculosis
T_H1	T helper 1
TNFα	Tumor necrosis factor alpha
TNFRp55	p55 TNF receptor
TLR	Toll-like receptor
TRAIL	TNF-related apoptosis inducing ligand
T_{reg}	Regulatory T cells
VEGF	Vascular endothelial growth factor
WT	Wild-type
WHO	World Health Organization

INTRODUCTION

1. Tuberculosis

Tuberculosis (TB) has plagued humankind worldwide for thousands of years. Besides archaeological evidences that TB was already present in Egyptian mummies, the climax of the TB epidemic occurred during the end of the XVIII century and the beginning of the XIX century, by the time of industrial revolution. Living and working in manufactures cities was terrible due to the overcrowded dwellings where sanitation and hygiene were absent. No wonder that TB was responsible for up to 25% of deaths in Europe. In the beginning of the XX century, new cases of TB began to fall as living standards (housing, nutrition, and income) improved, just before the advent of antituberculosis drugs. Despite the discovery of antituberculosis drugs more than 60 years ago, TB still remains a major global health problem [1-3]. In 2013, there were an estimated 9.0 million new cases of TB, and despite being in most instances, a curable disease, 1.5 million people died in 2013 due to TB. Although all countries are affected, 85% of cases occur in Africa (29%) and Asia (56%), while India and China alone represent 35% of TB cases (Fig. 1). TB is highly connected with the human immunodeficiency virus (HIV). People infected with HIV represent over 10% of annual TB cases and are up to 37 times more likely to develop TB than HIV-negative individuals [1, 4, 5].

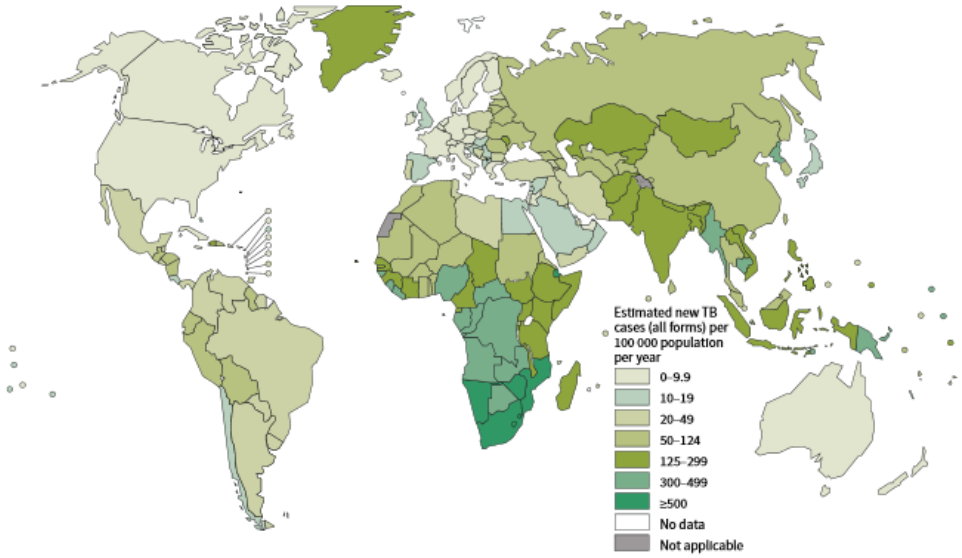

Figure 1 - Estimated TB incidence rates by country in 2013. Adapted from WHO [1](http://www.who.int/topics/tuberculosis/en/)

1.1. Epidemiology of *M. tuberculosis*

TB disease is mainly caused by the slow-growing acid-fast bacillus *Mycobacterium tuberculosis* (*M. tuberculosis*), identified by the Nobel Prize laureate, Robert Koch in 1882. According to estimates by the World Health Organization (WHO), one-third of the world's population is infected with *M. tuberculosis*, but remains asymptomatic and noninfectious– defined as latent TB. In 90% of the cases, the infection will not lead to active disease, while the other 10% will develop active disease in their lifetime [3, 4]. The *M. tuberculosis* is primarily transmitted by the respiratory route, through the inhalation of aerosolized droplets that carry the bacteria. TB is predominantly a disease of the lung and for that reason pulmonary TB is the most common, accounting for 70% of the cases. However, it can cause disease in other organs, including lymph nodes, bone and meninges, thereby causing extra pulmonary disease [6, 7].

1.2 *Mycobacterium* genus

The genus *Mycobacterium* includes more than 150 species that reside in a wide variety of habitats [8]. Among these species, the great majority are non-pathogenic environmental organisms, although this genus also contains important human pathogens. *M. tuberculosis complex* includes *M. tuberculosis, M. africanum, M. canetti, M. bovis* and *M. microti*, and these are all agents of TB, being the leading cause of death from a curable infectious disease in world. *M. leprae* and *M. ulcerans* are the causative agents of leprosy and buruli ulcers, respectively. These are, respectively, the second and third most common mycobacterial infections in humans, after TB [9, 10]. However, while TB, leprosy and buruli ulcers are specific diseases caused by specific mycobacteria, other mycobacteria are usually referred simply as atypical mycobacteria or nontuberculosis mycobacteria (NTM). According to current taxonomy, the NTM include more than 90 known species, however, about one third has been associated with human and animal diseases. Among the NTM, the *Mycobacterium avium* complex (MAC) attracts serious attention. The MAC comprises a group of closely related species: *Mycobacterium avium* (*M. avium*) and *M. intracellulare*. MAC is probably the most common cause of disease from NTM in most regions of the world. MAC is extremely widespread in numerous environmental sources, including soil, residential and hospital water systems, public drinking and potable water sources [11, 12]. In the last years of the 20th century, the *M. avium* infection became particularly relevant due to the close connection with the acquired immune deficiency syndrome (AIDS) patients. *M. avium* is an opportunistic infectious agent that mostly affects patients with underlying conditions that compromise immunity. In fact, *M. avium* is frequently found in AIDS patients. The HIV

infection leads to a progressive reduction of $CD4^+$ T cells that is correlated with the increasing risk of *M. avium* infection. The patients with advanced HIV disease ($CD4^+$ T cells count <50 cells/μL) have higher risk of developing *M. avium* infection. The risk does not appear to vary according to the gender, ethnicity or route of transmission [13, 14].

1.3 Immune responses to mycobacterial infections

1.3.1 Initial events following the mycobacterium infection

In humans, the most common routes of infection by *M. avium* are either through the intestinal tract, causing rapidly disseminating infections, or by the inhalation of droplets containing the bacillus, which slowly disseminate to other organs. Following the establishment of pathogenic *Mycobacterium* spp (including *M. avium*) infection, the bacilli are phagocytosed mainly by resident macrophages but also by neutrophils and dendritic cells (DCs). After successfully infecting the host, the lifestyle of *M. avium* is identical to that of other pathogenic mycobacteria. This process triggers a pro-inflammatory and anti-inflammatory response that induce the production of cytokines and chemokines, a stimulation of phagocyte antimicrobial activities and the recruitment of other cell types from neighboring blood vessels, which leads to the granuloma formation (which will be discussed later) [6, 7]. As previously described, the bacteria enter the host, and three outcomes are possible: (i) the immune system immediately destroys the mycobacteria (rare); (ii) the balance between the immune responses and the bacteria growth leads to the formation of the granuloma, preventing the dissemination of the mycobacteria - latent state; (iii) the infection leads to disease (this frequently occurs in immunocompromised individuals) – active disease [15, 16]. Despite the involvement of DCs and natural killer (NK) cells in the innate immune response against the mycobacteria infection, macrophages play the pivotal role in the resistance against the mycobacteria infection.

1.3.2 Recognition of the mycobacteria by macrophages

The immune system has the ability to detect and eliminate invading pathogenic microorganisms by discriminating between “self” and “non-self”. The innate immune system detects non-self through the pattern recognition receptors (PRR), which can recognize conserved molecular structures found in microbes. Therefore, phagocytosis of mycobacteria by macrophages is a prelude to microbial killing. The internalization of mycobacteria by macrophages is mediated by a diverse array of receptors: type A scavenger receptors, complement receptors (CR3 and CR4), mannose or Fcγ receptors.

Apart from phagocytosis, some data have also shown the importance of the recognition of *M. avium* via the Toll-like receptor (TLR) playing a key role in the innate immunity. So far, thirteen TLRs have been identified in humans, and each appears to be required for responses to a different class of infectious pathogen [17, 18]. TLR-2 has been described as the main receptor for mycobacterial components [19]. Wang *et al*, described that *M. avium* infection induces TLR-2 mRNA expression and decreases TLR-4 mRNA expression in macrophages [20]. The analysis of TLR-2 deficient mice has shown an increase of susceptibility to *M. avium* compared with the C56BL/6 mice [21, 22]. Interestingly, despite the clear involvement of TLR-2, mice deficient in myeloid differentiation factor 88 (MyD88), an intracellular adaptor protein that transduces signals from most TLR, are even more susceptible to *M. avium* than TLR-2 deficient mice [22]. The highly enhanced susceptibility of animals deficient in MyD88 was indicative that multiple TLRs might be involved in the innate recognition of *M. avium* [23].

1.3.3 Phagocytosis

Upon mycobacteria internalization, a sequence of processes leads to the formation of cytoplasmic vacuoles called phagosomes, which encapsulate the engulfed bacteria. Normally, the phagosome maturation is a complex process that leads to the fusion of the phagosome with the lysosome, resulting in the phagolysosome. The lysosome is a complex vacuolar organelle that contains hydrolytic enzymes capable of degrading the phagocytized material in the phagolysosome structure [24]. These enzymes are active at the optimally acidic pH (4.5 – 5.0) maintained within the lysosome, but not at the neutral pH of the cytosol [25]. The lysosome is, in fact, the most acidic organelle in humans [26]. The acidic environment results from the action of the membrane adenosine triphosphate (ATP)-dependent proton pumps, which actively transport protons into the lysosome from the cytosol [26, 27]. However, viable and virulent mycobacteria have the ability to prevent phagosomal maturation, by inhibiting the phagosome-lysosome fusion [28, 29]. Thus, through this mechanism mycobacteria can adapt to the intracellular environment of the macrophage, creating a niche for survival, which prevents the acidification of the phagocytic vacuole. The normal *M. avium* phagosomal environment is between pH = 5.8 to 6.1 and the pH optimal for *M. avium* survival is 6.0. This collectively suggests that the low acidic environment encountered by *M. avium* within macrophages favors its survival [25, 30].

However, the activation of macrophages causes a dramatic increase in the resistance against *M. avium*, leading to the maturation of mycobacterial phagosomes [31-33]. While unactivated macrophages have low microbicidal activity and express low levels of major histocompatibility complex (MHC) class II molecules, an activated macrophage shows

increased microbicidal activity through the improvement of killing mechanism and it is transformed into a potent antigen-presenting cell (APC) [33, 34]. Infected macrophages can produce numerous cytokines, namely, tumor necrosis factor alpha (TNFα) and interleukin – 12 (IL-12). These cytokines can act in concert to drive an interferon gamma (IFNγ) response from T helper type 1 (T_H1) and NK cells. IFNγ plays a major role in the activation of macrophages [35]. Several *in vitro* studies suggest that mycobacterial phagosomes are shifted from an early to a late endosomal stage of the phagosome maturation by macrophage activation, which is associated with a reduction in mycobacterial growth and viability [36, 37]. Notably, experiments using IFNγ deficient mice showed an exacerbation of *M. avium* infection [38, 39]. These findings suggest that resistance to mycobacteria requires the secretion of IFNγ, which leads to the activation of macrophages and consequently to the control of the infection.

1.3.4 Killing mechanisms

Among the antimicrobial mechanisms of the macrophage, those involving oxidative damage such as: the respiratory burst with production of reactive oxygen species (ROS) and nitric oxide (NO), have proven to be important mechanisms in the killing of many pathogens. In fact, these two systems act synergistically in killing many microbes. These mechanisms are considered the major players in the growth control of intracellular parasites. However, numerous studies highlighted the existence of antimicrobial activity, which is not dependent of NO and ROS generation. In fact, the use of $p47^{phox}$ (component of the NADPH oxidase) deficient mice, have shown that the respiratory burst is not required for the control of *M. avium* [40, 41]. Doherty and Sher showed that inducible nitric oxide synthase (iNOS) deficient mice were resistant to *M. avium* infection [42] and that at later stages of infection they were even more resistant [43]. With a similar approach, studies with *Salmonella* and *Listeria* using double knockout mice deficient in the generation of ROS and iNOS showed that macrophages were able to kill the bacteria [44]. These findings suggest the existence of ROS and NOS-independent antimicrobial mechanisms.

The deprivation of essential nutrients arises as a potential mechanism to limit intracellular growth of *M. avium*. Early studies on the genetics of susceptibility to infection highlighted the role of the gene natural resistance associated macrophage protein 1 (Nramp1) or solute carrier family 11a member 1 (Slc11a1) in the control of *M. avium* infection in mice [40, 45]. Nramp1 is a transmembrane protein expressed in endosomal and phagosomal membranes of macrophages, and has the ability to affect the capacity of the host to control intracellular replication, presumably by depriving the access to iron by the pathogen [46, 47].

Consequently, a strong dependence of the infection severity upon the presence of functional *versus* dysfunctional Nramp1 allele it has been demonstrated in mice [48, 49].

1.3.5 Cytokines

Cytokines are important mediators and regulators of the immune response against all pathogens. The interaction between the pathogens and cells of the immune system strongly induces the secretion of cytokines which are crucial in innate defense and in determining the subsequent adaptive response. In this section, the roles of various cytokines involved in the response to *M. avium* are discussed.

IFNγ plays a key role in the control of *M. avium* infection. This cytokine is mainly produced by $CD4^+$ T cells [50] and NK cells (Fig. 2). It is now known that the innate lymphocytes, γδ T cells, natural killer T cells (NKT) and $CD8^+$ T cells can also produce IFNγ in response to mycobacterial stimulation. IFNγ plays a crucial role in the activation of macrophages, promoting the production of NO and other intermediates, that results in mycobacterial growth control. In fact, *in vivo* neutralization of IFNγ exacerbates *M. avium* infection [38, 39] and IFNγ deficient mice are more susceptible to the infection [42, 51].

TNFα also plays a major role in the initial and long-term control of *M. avium* infection. *M. avium* induces TNFα secretion by macrophages, neutrophils, DCs and T cells. TNF is important in early response by activating macrophages (Fig. 2) as well as cell recruitment to the site of infection. The important role played by TNFα during *M. avium* infection was demonstrated through the exogenous administration of TNFα *in vitro*, which led to *M. avium* elimination [52, 53]. In the other hand, the neutralization of TNFα led to exacerbation of *M. avium*[54] and it was also shown that TNFα deficient mice succumbed to *M. avium*[53, 55].

IL-12 is induced in response to mycobacteria by macrophages and DCs. Subsequently, IL-12 stimulates the production of IFNγ by immune cells, in particular NK cells and helper T cells (Fig. 2) [56]. The production of IFNγ has a very powerful effect in enhancing the ability of phagocytic cells to produce IL-12. This cytokine also enhances the production of IFNγ, creating a positive reinforcement loop [57]. IL-12 also drives an adaptive cellular response, inducing T_H1 differentiation, which become a major source of IFNγ. Not surprisingly, IL-12p40 deficient mice are highly susceptible to *M. avium* infection and the neutralization of IL-12 exacerbated *M. avium* infection. It has also been reported that in the absence of IL-12, IFNγ responses were drastically reduced and upon exogenous administration of recombinant IL-12, IFNγ responses were enhanced leading to increased protection [58, 59]. Additionally, TLR-2 and CD40 appear to be required for an optimal IFNγ-dependent protective immune response to *M. avium*. Both TLR-2 and CD40 play an important role by generating optimal levels of IL-12p40 [21, 60].

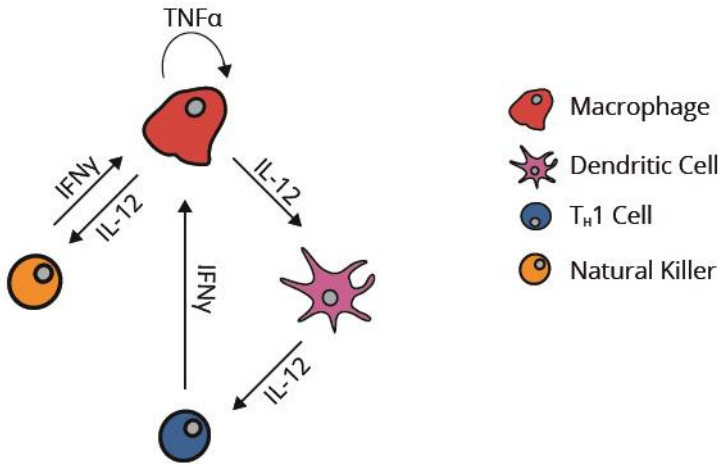

Figure 2 – Classical activation of macrophages. Macrophages can produce numerous cytokines, namely TNFα and IL-12, which are essential for macrophage activation. IL-12 has the ability to stimulate the production of IFNγ by NK cells and T_H1 cells. IFNγ play a major role in the activation of macrophages. Activated macrophages will enhance the production of IFNγ, creating a positive reinforcement loop.

1.3.6 Other innate and adaptive immune cells

There are other cells that participate in the innate response besides macrophages, such as DCs, NK cells, and neutrophils.

The role played by NK cells in mycobacterial infections is not clear, however there are several studies demonstrating a role for this cell population. It is known that NK cells are able to secrete cytokines such as IFNγ, a major modulator of *M. avium* infection. The role of NK cells during *M. avium* infection was demonstrated through the depletion of NK cells by using an anti-NK1.1 monoclonal antibody. The results obtained in this *in vivo* model showed an uncontrolled multiplication of *M. avium* in C57Bl/6 mice [61]. By using *in vitro* assays, it has been demonstrated that NK cells interact with macrophages and this leads to a reduction in mycobacterial proliferation [62].

The involvement of neutrophils in mycobacterial infections has been discussed controversially in the literature in the past few years [63, 64]. Since neutrophils only ingest mycobacteria in the first hours of infection and since the infection will become chronic, it is unlikely that neutrophils kill *M. avium*. However, the neutrophils as a cell type are more complex than the simple ingestion and killing [65]. The neutrophils play an important role in determining the immune response and also in cooperating with other cell types to improve the effector responses of the immune system. The importance of neutrophils in the protective

response was shown by the depletion of neutrophils using a monoclonal antibody which led to the exacerbation of the infection [63, 64]. Infected neutrophils might be involved in the recruitment of a protective type 1 response through the secretion of chemokines and cytokines (such as IL-12 and TNFα) [64]. More recently, it has been suggested that neutrophils might be involved in the adaptive immune response by crosstalk with DCs in order to increase mycobacterial antigen presentation [65, 66].

DCs are specialized in the presentation of antigen to T cells. Mycobacteria infected DCs migrate to the lymph nodes under the influence of IL-12p40, IL-12p70, CCL19 and CCL21 to drive naïve T cells differentiation toward a T_H1 phenotype. DCs are the major source of IL-12, an essential cytokine in the production of IFNγ by immune cells ($CD4^+$ T_H1 cells and NK) [6, 67]. The role of DCs in the mycobacterial infection was demonstrated through the depletion of DCs. Tian *et al*, have shown the importance of DCs in the initiation of the adaptive T cell response, since the absence of DCs led to a delay of $CD4^+$ T cell response, which consequently led to the exacerbation of infection [68].

Early recognition of *M. avium* is crucial to bacterial growth control. However, protective immunity against *M. avium* also requires efficient cell mediated immune responses by $CD4^+$ and $CD8^+$ T cells. This section will summarize how T cells contribute to protective immunity against *M. avium*. It is clear that $CD4^+$ T cells play a crucial role in the control of infection by atypical mycobacteria, such as *M. avium*, being the major producers of IFNγ. The secretion of this cytokine leads to activation of mycobacterium-infected macrophages, inducing NO and RNS production but also IL-12 and TNFα, which contribute to the control of the pathogen. *M. avium* is opportunistic pathogen infecting immunocompromised individuals such as AIDS patients with low $CD4^+$ T cells counts [6, 11]. The fact that a severe depletion of the $CD4^+$ T cells in AIDS patients favors the establishment of infection by this mycobacteria, suggests that T cells play a major role in the host defense against *M. avium* infection in humans. *In vivo* experiments, using $CD4^+$ T cell deficient mice confirmed the requirement of $CD4^+$ T cell in the *M. avium* growth control [69]. Despite substantial evidences that $CD4^+$ T cells are crucial for an effective defense against *M. avium*, the role of $CD8^+$ T cells remains unclear and does not appear to influence the control of *M. avium* infection. In a $CD8^+$ T cell deficient mice the bacterial load did not show any difference compared to C57BL/6 mice [69]. Another study with a β2-microglobulin deficient mice confirmed the negligible role played by the MHC class I-restricted $CD8^+$ T cells [35, 70].

1.4 Immunopathology of mycobacteria

After *M. avium* recognition and up take by the resident macrophages, the bacteria can interfere with key antimicrobial mechanisms and start to replicate intracellularly. Infected macrophages will produce a range of cytokines and chemokines that will attract additional monocytes, neutrophils and DCs. Infected macrophages or DCs can migrate to the draining lymph node under the influence of IL-12p40 and IL-12p70 and serve as APC to drive naïve T cell differentiation towards a T_H1 phenotype. Protective antigen-specific T_H1 cells migrate back to the infection site and produce IFNγ, thereby leading to macrophage activation [6, 15]. After arriving at the site of infection, the immune cells of both innate and adaptive immunity form the classical granuloma. Granulomas are well-organized aggregates of immune cells, namely heavily infected macrophages and stimulated macrophages which have differentiated into multinucleated giant cells, epithelioid cells, foamy (lipid-rich) macrophages and neutrophils, surrounded by a ring of lymphocytes, largely $CD4^+$ T cells, but also $CD8^+$ T cells, B cells, DCs, NK cells and by fibroblasts, which create a peripheral fibrotic capsule [6, 71, 72]. The mycobacterial granuloma contributes to host protection through different functions. The granuloma's main function is to constrain and prevent the dissemination of the mycobacteria, concentrating the immune response to a limited area. Furthermore, T cell-activated macrophages can lead to the control of bacterial growth. Granulomas also restrict tissue damage by shielding the surrounding tissue from the chronic inflammation. The mycobacteria can persist within the granuloma structure for decades in a latent state. This latent state is characterized by the control of bacterial proliferation through the balance of immune responses [71, 73].

For some unknown reasons, mycobacteria can reactivate due to a deregulation of immune responses. This will lead to granuloma progression and no control of mycobacterial growth. In such situations, the granuloma is no longer able to contain the bacteria and these lesions grow to macroscopic sizes and may evolve to show areas of central necrosis. This type of lesions is present not only in *M. avium* infection but also in *M. tuberculosis* infection. In fact, the hallmark of human TB is the caseating granuloma with an amorphous acellular core of necrotic material that resembles "cheese" (with *caseum* being the Latin word for cheese). The accumulation of caseum in the center of the granuloma leads to the collapse of the granuloma center, releasing the virulent bacilli to other parts of the tissue where more lesions will be formed [15, 16, 73].

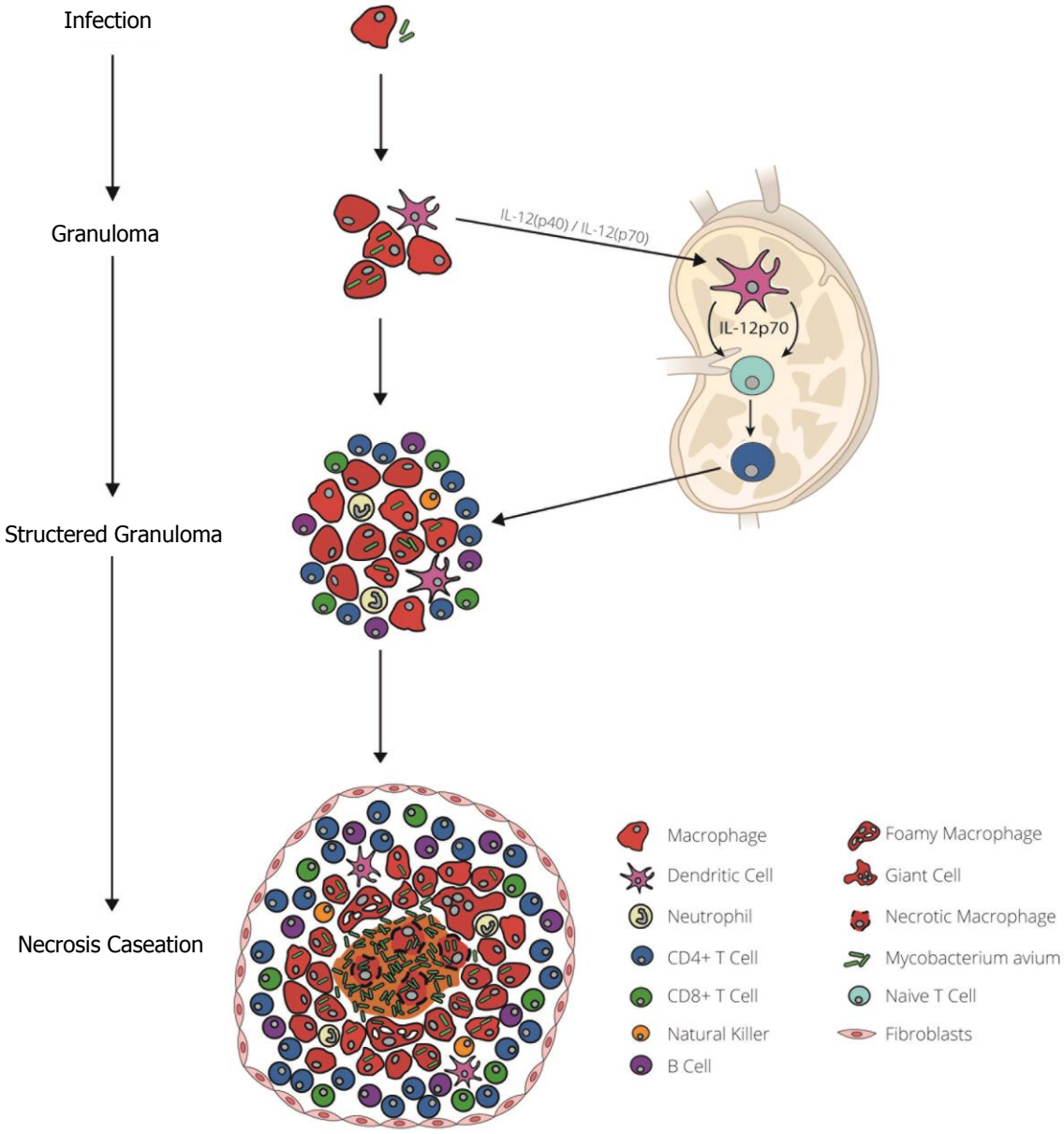

Figure 3 – Sequence of events following the infection with *M. avium*. The infection starts with the phagocytosis of the bacteria by tissue macrophages. Upon the contact with *M. avium*, DCs can migrate to the lymph nodes under the influence of IL-12p40 and IL-12p70 to drive naive T cell differentiation toward a T_H1 phenotype. T_H1 cells migrate back to the infection site to form the classical granuloma.

1.4.1 Granuloma necrotizing models

Some studies using knockout mice infected with *M. avium* have clearly shown the importance of T cells in the development of protective immunity against mycobacterium infections. These studies also showed that although the assembly of a granuloma may occur

in the absence of T cells, the granuloma is poorly structured. More interesting, neither nude nor CD4 deficient mice exhibited central necrosis. Morphologic analysis showed smaller lesions and extensive accumulations of infected macrophages and few lymphoid cells. On the other hand, the CD8 deficient mice present central necrosis similar to that found in C57Bl/6 mice [69, 74].

The role of IFNγ in granuloma formation was demonstrated by Flórido *et al* using IFNγ deficient mice infected with *M. avium* [69]. The histological analysis showed severe deficiencies in the formation of granulomas and the absence of necrosis. No granulomas were found in IFNγ deficient mice, but instead some accumulations of macrophages heavily infected with *M. avium* were identified [69, 74]. The importance of IFNγ inducers, such IL-12, IL-6 and CD40 in granuloma formation is also described in the literature. The IL-12 or CD40 deficient mice also showed lack of cellular infiltration and absence of necrosis as was observed using IFNγ deficient mice. On the other hand, IL-6 deficient mice showed well-structured granulomas, however these consisted of smaller lesions with less evidence of necrosis compared to WT mice [23, 69, 74].

To address the role of TNF in the formation of granulomas, mice with genetic ablation in TNF [75], p55 TNF receptor (TNFRp55) [69, 76] or TNF-related apoptosis inducing ligand (TRAIL) [77] were used. The action of TNF is mediated by two different receptors, the type I and type II TNF receptors, also known as p55 and p75 respectively [78]. The TNFRp55 has been shown to be important in the control of TB infection in mice [79]. On the other hand, TRAIL is expressed by different cell types and is capable to bind to death receptors, which contain a death domain in the intracellular region to induce cell apoptosis [80, 81]. It was shown that TNFRp55 is not required for the assembly of the granuloma and even in the absence of TNF, TNFRp55 or TRAIL necrosis still appeared [75-77].

Curiously, the same observation was made in certain inbred strains of mice such as BALB/c or DBA/1. In fact, despite similar levels of *M. avium* proliferation found in these strains compared with C57BL/6 mice, the development of granuloma necrosis it was not observed. These experiments have shown the role of complement component C5 on the development of the granuloma progression, since DBA-1 strain were C5 deficient [82]. The lack of C5 led to a diminished expression of chemokines and cytokines, which probably affected the recruitment of leukocytes [83, 84]. These models provided evidence that complement component C5 is required not only for the efficient organization of granuloma but also for the development of the granuloma necrosis [82].

1.5 *Mycobacterium avium* study model

The mouse model offers the best tool for the study of development and progress of necrotic granulomas. Nevertheless, normal mice infected with *M. tuberculosis* develop granulomas that seldom undergo necrosis. These granulomas are poorly organized and exclusively cellular; they lack fibrosis or hypoxia; the bacterial counts remain at a relatively high but apparently controlled level throughout the course of the disease; and all the mice ultimately die of progressive infection. This does not readily recapitulate the pathology seen in the human disease [6, 69, 73]. However, although lacking a good model of TB in mice, TB lesions can be found in guinea-pigs and rabbits infected with low-doses of virulent *M. tuberculosis*. Unfortunately, this can be very restrictive in the experimental point of view, since the availability of these species is small [85]. The Appelberg group has developed a granuloma necrosis model that mimics the human pathology of *M. tuberculosis.* Using a low dose (10^2 colony-forming units (CFUs)) inoculum of a highly virulent strain of *M. avium* (ATCC 25291) in C57BL/6 mice, it is possible to observe the development of granuloma necrosis in the lungs and liver after approximately four months of infection. This type of infection is characterized by the formation of small lesions that grow progressively into large granulomas that undergo central necrosis, which bears many resemblances with the lesions found in humans infected with *M. tuberculosis* or *M. avium*. Curiously, the same mice infected with the same strain of *M. avium* but with a higher dose (10^6 CFUs) never developed this type of lesion [69, 86].

2. Hypoxia and mycobacteria pathology

In an effort to better understand the mechanisms underlying the development of caseous necrosis, some studies have shown different evidences of severe hypoxic regions at the center of necrotic granulomas. It was already demonstrated that *M. tuberculosis* granulomas in guinea pigs, rabbits and nonhuman primates became hypoxic [85]. In contrast, severe hypoxia was not demonstrated in pulmonary lesions of C57BL/6 mice infected with *M. tuberculosis* strain H37Rv. However, when using C57BL/6 mice infected with *M. avium* strain TMC724 hypoxic granulomas were observed[87]. However, both studies have shown hypoxia by two different methods: the direct measurement of the partial pressure of oxygen (pO_2) using a flexible Clarke type electrode catheter, or by using the pimonidazole marker providing immunohistochemical evidence of hypoxia. Pimonidazole hydrochloride is an imaging agent that is activated under hypoxic conditions in mammalian tissue [85, 87]. Recently, through a noninvasive positron emission tomography (PET) imaging of live animals, hypoxic lung necrotic granulomas in C3HeB/FeJ mice infected with *M. tuberculosis* strain H37Rv

were demonstrated. In this technique, each mouse was injected via the tail vein with Copper(II)-diacetyl-bis(N^4-methyl-thiosemicarbazone), which in normoxic cells is reduced while in live cells in hypoxia is retained [88].

2.1 Hypoxia-inducible factor

The maintenance of oxygen homeostasis is an essential process in mammalian cells. The understanding of the molecular mechanism underlying this fundamental aspect of cell biology has started only few years ago [89, 90]. When the balance between oxygen supply and demand is affected, tissue hypoxia and cell death can rapidly occur. Hypoxia is induced not only as a global consequence of a decreased oxygen tension, but also locally at sites of inflammation, tissue ischemia and injury, and solid tumor growth [91, 92]. Therefore, adaptation to hypoxia is a vital survival mechanism in mammalian cells. These cells have the ability to adapt to conditions of hypoxia through the induction of the expression of several genes. The hypoxia-inducible factor-1 alpha (HIF-1α) has emerged as a master regulator, mediating a wide range of physiological and cellular mechanisms indispensable to adapt to hypoxia. HIF-1α is directly involved in angiogenesis [93], erythropoiesis [94], cell growth and differentiation [95], survival and apoptosis [96].

Under normoxic conditions, HIF-1α has a very short half-life. At normal concentrations of O_2, HIF-1α is suppressed by hydroxylation of two prolyl residues (Pro-402 and Pro-564). This modification allows the interaction with the von Hippel-Lindau tumor suppressor protein (pVHL). pVHL is the recognition component of E3 ubiquitin ligase complex that targets HIF-1α for ubiquitination and proteasomal degradation. Under hypoxic conditions, prolyl hydroxylation is suppressed and HIF-1α escapes from proteasomal degradation. Thus, HIF-1α becomes stabilized and translocates from the cytoplasm to the nucleus, where it dimerizes with HIF-1β. The HIF complex formed becomes transcriptionally active, binding hypoxia-response elements (HREs) [91, 97]. Classical HIF-1α target genes include the vascular endothelial growth factor (VEGF) [98], erythropoietin [94], glucose transporters [99] and transferrin [100].

Besides HIF-1α, HIF-2α is also involved in the regulation of physiological and cellular mechanisms in the hypoxia adaptation[101]. The HIF-2α and HIF-1α subunits are structurally and functionally similar, since they also have the two prolyl residues, which are hydroxylated in normoxia, and are targeted for degradation by VHL ubiquitin E3 ligase complex. In hypoxic conditions, the inhibition of hydroxylation results in stabilization of HIF-2α which consequently translocates to the nucleus, where it dimerizes with HIF-1β, resulting in the HIF-2 complex, which transactivates HRE-target genes [102,103]. A number of studies also

showed that HIF-2α plays an important role in regulating macrophage responses to hypoxia, however there is some debate about which form of HIF is the most important in the regulation of macrophages in hypoxic conditions [104, 105].

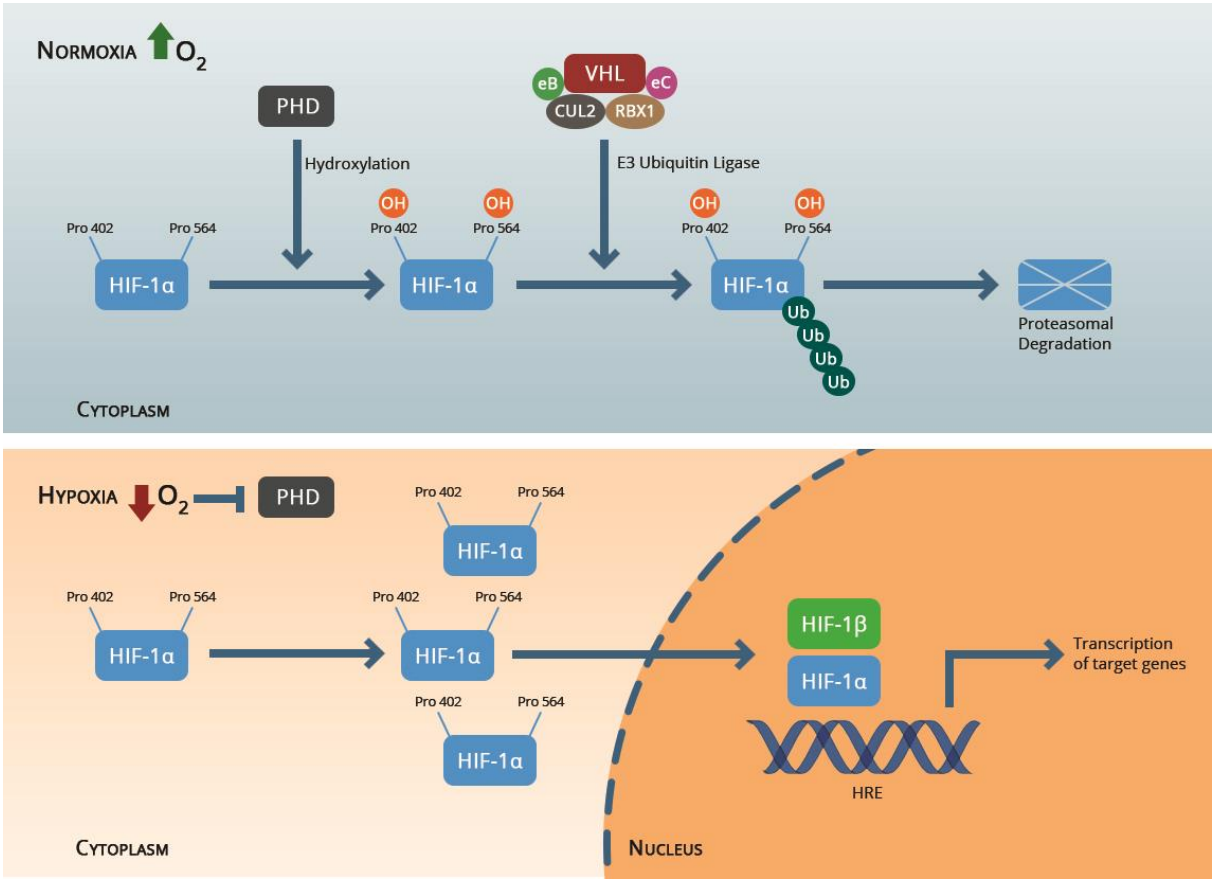

Figure 4 – HIF-1α pathway. Under normoxia the HIF-1α is rapidly degraded. In this condition, HIF-1α is suppressed by hydroxylation and target for proteasomal degradation. During hypoxia, HIF-1α becomes stabilized and is translocated to the nucleus, where the HIF complex becomes transcriptionally active.

2.2 Immune system and hypoxia

Microenvironmental conditions are frequently encountered in injured tissues and are characterized by low levels of oxygen. This is probably due to a combination of some factors including the excessive oxygen consumption by highly metabolically activated resident cells, but also by infiltrating immune cells. It has also been shown that chronic inflammation leads to a marked deregulation of vasculature [106, 107]. Thus, the immune cells that are recruited to these inflammation sites need to adapt to hypoxia in order to remain functionally active. Lewis and colleagues showed that hypoxic conditions profoundly affect a broad range of

myeloid cell properties *in vitro*, e.g., phagocytosis, cell surface marker expression, secretion of cytokines, chemokine receptor levels, adhesion, migration and cell survival[108]. To maintain their biological activities in hypoxia, immune cells need to shift their metabolism to anaerobic glycolysis to generate ATP. Some studies in hypoxia environment have shown that inhibition of glycolysis can directly inhibit ATP production and subsequently, myeloid cell properties as diverse as adhesion, extravasation, motility and invasion. Recently, HIF-1α has arisen as a key regulator of glycolysis and immune functions [106, 109].

2.3 HIF-1α function in immune cells

The crucial role of HIF-1α in immune cell functions using different conditional knockout mice lacking HIF-1α has been demonstrated in several studies. The influence of HIF-1α in the innate immune system is relatively well established and a role in the adaptive immune system has recently been proposed [90, 109].

The absence of HIF-1α in cells from the myeloid lineage showed a profound impairment of myeloid cell aggregation, motility, invasiveness, and bacterial killing [109]. In fact, Anand and colleagues have shown by *in vitro* assays, that HIF-1α activation led to an increase of the phagocytic activity and to bacterial killing under hypoxic conditions, when compared to normoxic conditions [110]. HIF-1α is strongly stimulated under bacterial exposure and has the ability to regulate the production of key immune effectors molecules, including NO and TNFα [111]. Nevertheless, studies using conditional knockout mice lacking HIF-1α in T cells [112], B cells [113], neutrophils [114] or DCs [115], have demonstrated an important influence of HIF-1α in the immune function. The loss of HIF-1α in DCs led to an impairment of DCs migration from the periphery, tissue and blood circulation and consequently, to a decrease of DCs ability to stimulate T cells. In addition, the upregulation of HIF-1α during hypoxic conditions led to enhanced apoptosis of immature DCs [90, 115, 116]. In the adaptive immune response, HIF-1α works as a key metabolic sensor, regulating the differentiation of T_H17 and regulatory T cell (T_{reg}) [117, 118]. The absence of HIF-1α in T cells has shown the induction of higher levels of pro-inflammatory cytokines in response to T cell receptor activation [112]. Surprisingly, it was found that under normoxia conditions HIF-1α complex was also upregulated. Apparently non-hypoxic stimuli as glucose [119], lipopolysaccharide (LPS) [120], TNFα [121] IFNγ [122] and nuclear factor- kappa B (NF-κB) [123] are possible modulators of HIF-1α transcription and therefore able to influence the expression of hypoxic genes.

3. Aims

The development of necrosis is a crucial mechanism in the progression of *M. avium* infection, however still poorly understood. Therefore, the better understanding of necrotizing mechanism and how granulomas can control the *M. avium* infection is needed. Thus, the main goal of this thesis is to understand the mechanism underlying caseous necrosis. Since, recently, some literature has described the presence of hypoxia at the center of necrotic granulomas and since necrosis only occurs when granulomas increase in size, we suggest that necrosis is a direct consequence of the absence of oxygen. Here, we show that granuloma increase in size and became less vascularized before the development of necrosis. We evaluate the impact of lacking HIF-1α in myeloid cells and the quantification of HIF-1α during *in vivo M. avium* infection.

METHODS

Mice

C57BL/6 wild-type (WT) mice were bred in our facilities from a breeding pair purchased from the Harlan Iberica (Barcelona, Spain). HIF-1α deficient C57BL/6 mice (HIF-1α$^{-/-}$) were obtained in our facilities after back-crossing the B6.129-Hif1α^{tm3RSjo}/J and the B6.129P2-Lyz2$^{tm1(cre)Ifo}$/J (LysMcre mice) strains, both from the Jackson Laboratory (Bar Harbor, ME, USA), based on the Cre-lox system. Briefly, the B6.129-Hif1α^{tm3RSjo}/J strain has *loxP* sites on either side of exon 2 of the HIF-1α gene and LysMcre mice have a Cre recombinase inserted into the first coding ATG of the lysozyme 2 gene (Lyz2). The crossing of these two strains of mice resulted in the deletion of the HIF-1α gene only in myeloid cells including monocytes, mature macrophages and granulocytes. The first generation obtained was HIF-1α heterozygous; the second generation obtained was HIF-1α heterozygous (single knockout) and homozygous (double knockout). After confirming the genotype of each animal, the double knockouts were successively crossed to obtain an offspring of HIF-1α double knockouts (third generation). The genotyping was performed according to the genotyping protocols database from Jackson Laboratory (Bar Harbor, ME, USA).

All mice were kept in our animal facilities in high-efficiency particular air (HEPA)-filter-bearing cages under 12 hours light cycles, and fed autoclaved chow and water *ad libitum*. All mice were used at 8-12 weeks of age. All experiments were performed in accordance with the National and European guidelines and approved with by the IBMC.INEB Animal Ethics Committee.

Bacteria

The highly virulent *M. avium* strain (ATCC 25291 SmT) was obtained from the American Type Culture Collection (ATCC) (Manassas, VA). Mycobacteria inoculum was obtained from a smooth-transparent morphotype colony, grown in Middlebrook 7H9 medium (Difco, Detroid, MI) containing 0.04% Tween-80 (Sigma, St Louis, MO) and supplemented with 10% albumin-dextrose-catalase (ADC) at 37ºC until the mid-log phase of growth. Bacteria were harvested by centrifugation and resuspended in a small volume of saline containing 0.04% Tween 80. The bacterial suspension was sonicated with a Branson sonifier (Danbury, CT) in order to disrupt bacterial clumps and stored in aliquots at -80ºC until bacterial load determination and use in *in vivo* infection. Before inoculation, bacterial aliquots were thawed at 37ºC and diluted in saline to the desired concentration ($5x10^2$ CFU/ml).

In vivo infection

C57BL/6 and HIF-1α$^{-/-}$ mice were infected with 10^2 CFUs of *M. avium* strain 25291 through a lateral tail vein. Infected mice were euthanized (isofluorane plus cervical dislocation) at different times points after infection and the livers, spleens and lungs were aseptically collected. A portion of the liver was fixed in 4% paraformaldehyde for histological analysis. Spleen and liver samples were collected in Dulbecco's modified Eagle's tissue culture medium (DMEM; Life Technologies, Paisley, UK) containing 10% fetal bovine serum (FBS; Life Technologies), 5% glutamine and 1% penicillin/streptomycin (P/S).The bacterial load was determined in tissue homogenates from infected mice, by serial dilutions in distilled sterile water with 0.05% Tween and plated, in duplicate, onto Middlebrook 7H10 agar medium (Difco, Detroid, MI) supplemented with oleic acid-albumin-dextrose-catalase (OADC). 7H10 plates were incubated for 10 days at 37 °C and the numbers of CFU were counted using a magnifying glass. The bacterial load was calculated taking into account the dilution factor and the final volume of the tissue homogenate.

Isolation of liver mononuclear cells

Liver mononuclear cells were isolated from the liver homogenate by density centrifugation. A single cell suspension was obtained from the liver by passing the organ through a 70 µm cell strainer (BD Biosciences, San Jose, CA). Liver cells were washed at least two times (500g, 10 minutes) with phosphate-buffered saline (PBS) until the supernatant got clear. After the last centrifugation, cells were resuspended in DMEM and gently layered in a falcon with density gradient reagent - *Histopaque 1083* (Sigma-Aldrich, Taufkirchen, Germany). After centrifugation at 1000g for 25 minutes at room temperature (RT) without acceleration or brake, liver mononuclear cells were recovered from the interphase between the histopaque and the DMEM. Cells were washed with DMEM to remove histopaque residues and liver mononuclear cells were finally resuspended in DMEM.

HIF-1α quantification

Liver mononuclear cells were fractionated into cytoplasmic and nuclear protein extracts using a cell fractionation kit according to the manufacturer's instructions (BioVision, Mountain View, CA). Total HIF-1α was quantified using the cytoplasmic extracts by a two-site sandwich enzyme-linked immunosorbent assay (ELISA) according to the manufacturer's instructions (R&D Systems, Minneapolis, MN). Positive controls were provided by the

manufacturer. All samples were assayed in duplicated. The values were normalized to the total liver mononuclear cell number isolated from each mouse.

IFNγ quantification

Spleen cell suspensions from infected and control mice were individually prepared using Potter-Elvehjem tissue homogenizer, resuspended in DMEM, supplemented with 10% fetal calf serum (FCS; Life Technologies). Erythrocytes were lysed by incubation of the cell suspensions with a hemolytic buffer (155 mM NH_4Cl, 10 mM $KHCO_3$, pH 7.2) for 5 minutes at RT. The cell suspensions were then thoroughly washed with Hanks' balanced salt solution (Life Technologies) and resuspended in DMEM with 10% FCS, 5% glutamine and 1% P/S. Cells were cultivated at a density of $2x10^5$ cells/well in a U-bottom, 96-well microtitre plate. Cells were incubated in triplicate in DMEM with 10% FCS with no further stimulus or stimulated with mycobacterial antigens (4 µg/ml) or concanavilinA (4µg/ml, Sigma).Supernatants from the cultures were collected after 72 hours of culture at 37ºC in a 7% CO_2 incubator and the IFNγ produced was quantified by the ELISA method using anti-IFNγ-specific affinity-purified monoclonal antibodies (R4-6A2 as capture and biotinylated AN-18 as detecting antibody). Finally, a standard curve was generated with known amounts of recombinant murine IFNγ (Genzyme, Cambridge, CA).

Flow cytometry

For the immunofluorescence staining, 10^6 cells were incubated in a 96-well plate with different combinations of the following monoclonal antibodies. Briefly, a mixture of fluorescein isothiocyanate (FITC) – conjugated anti-CD19 antibody (dilution 1:50), phycoerythrin (PE) – conjugated anti-CD3 antibody (dilution 1:80), V450 – conjugated anti-CD4 antibody (dilution 1:200) and V500 – conjugated anti-CD8 antibody (dilution 1:150) was used in order to identify the different lymphocyte populations; and a mixture of brilliant violet 510 (BV 510) – conjugated anti-CD11b antibody (dilution 1:100), brilliant violet 421 (BV 421) – conjugated anti-CD11c antibody (dilution 1:100), allophycocyanin (APC) – conjugated anti-Ly6G antibody (dilution 1:200), allophycocyanin with cyanin-7 (APC/Cy7) – conjugated anti-F4/80 antibody (dilution 1:80) and FITC - conjugated anti-DX5 antibody (dilution 1:200) to identify the myeloid cells as well as the NK cells. The monoclonal antibodies were diluted in PBS containing 3% FBS and 0.01% sodium azide (NaN_3). After 30 minutes of incubation at 4ºC in the dark, cells were washed twice in PBS/3%SBF/0.01%NaN_3, and fixed with paraformaldehyde 4% for 20 minutes at RT. Cells were washed once more in

PBS/3%SBF/0.01%NaN_3 and resuspended in PBS/3%SBF/0.01%NaN_3. All the antibodies were obtained from Biolegend except for V450-CD4 and V500-CD8 that were obtained from BD Bioscience. Single-stainings and unstained samples were used to calibrate the voltages for sample acquisition and for colour compensation on the flow cytometer. The acquisition of the spleen and liver mononuclear cells was performed using a FACS Canto II flow cytometer using BD FACSDiva software (BD Biosciences). Data were analyzed using FlowJo software (Tree Star, Ashland, OR). To determine the cell number of each cell population, the number of gated events was multiplied by the total cell number (counted using Kova chambers) and divided by the total number of events select by forward scatter (FSC) / side scatter (SSC) parameters.

Gating strategy

Cells were selected on the basis of FSC/SSC and the singlets were gated according to size *versus* the width. For the lymphocytes analysis we used CD19 as a marker of B cells and CD3 to label T cells. Inside this gate $CD4^+$ T and $CD8^+$ T cells were distinguished (Fig. 5A). For the myeloid analysis the first gate was made on $Ly6G^{high}/CD11b^+$ defined to be neutrophils. Another gate was made on $CD11b^+/Ly6G^-$ in order to identify other types of myeloid cells. $CD11b^+$ is expressed on monocytes, macrophages, neutrophils, DCs and NK. On the $CD11b^+$ gate we plotted the F4/80 against DX5 to distinguish the macrophages by the expression of $CD11b^+/Ly6G^-/F4/80^+/DX5^-$ and NK by the expression of $CD11b^+/Ly6G^-/F4/80^-/DX5^+$. Still on the $CD11b^+$ gate we identify DCs by the expression of $CD11b^+/Ly6G^-/CD11c^{high}/DX5^-$ (Fig. 5B).

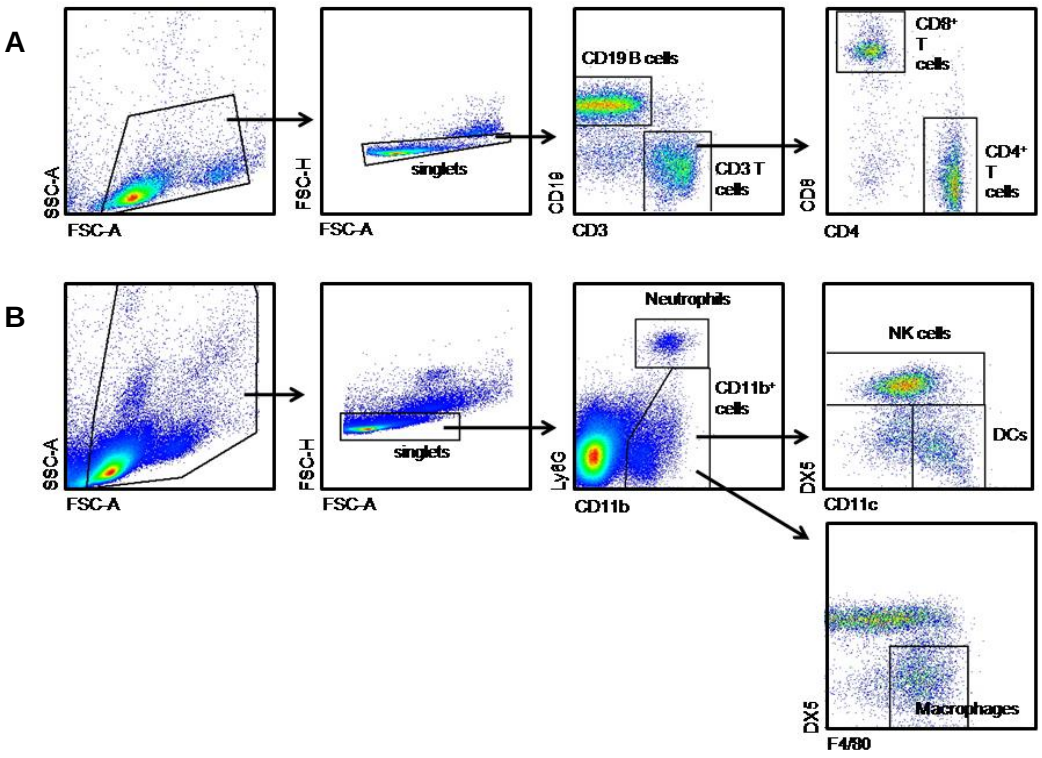

Figure 5 – Gating strategy – Spleen and liver cells were stained with different markers in order to identify different lymphocyte (A) and myeloid populations (B).

Histology

Portions of the organs from infected mice were fixed in buffered formaldehyde and embedded in paraffin. Sections were stained with haematoxylin and eosin, using a standard histological technique. For the detection of acid-fast bacteria, sections were stained by the Ziehl-Neelsen method.

Morphometric analysis of the granulomatous area

Histological sections of liver stained with haematoxylin and eosin (HE), from infected animals were captured using an Olympus CX31 light microscope equipped with a DP-25 camera (Imaging Software CellˆB, Olympus, Center Valley, PA). Random fields within each section under study were analyzed. The determination of granulomatous/cell infiltration area was done in a total tissue area ranged from 6 to 9 $x10^6$ μm^2, corresponding to a number of fields analyzed in each section between 5 and 6. The number of cellular infiltrates was the sum of all granulomatous/cell infiltration areas. It was analyzed one liver section per animal and measurements were done blind. To determine the liver area covered by granulomas, the

NIH ImageJ software program was used. The percentage of granuloma area was calculated for each mouse by dividing the sum of granulomatous areas by the total area of the liver section analyzed.

Immunohistochemistry

Sections were deparaffinized in xylene, and hydrated in an ethanol gradient (100%, 96% and 75%). The sections were next permeabilized in PBS containing 0.1% Triton X-100 and 0.1% Tween 20 (wash solution) for 5 minutes. Antigens were retrieved with 10mM sodium citrate buffer for 30 minutes at 96ºC. Endogenous peroxidase activity was blocked with 0.3% hydrogen peroxidase in methanol for 35 minutes at RT, followed by blocking the nonspecific antibody binding with normal horse serum (Vector Labs, Burlingame, CA; Dilution 1:50) in wash solution containing 5% BSA for 1 hour in a humid chamber at RT. Sections were incubated overnight at 4ºC with the following primary antibodies in wash solution: rat IgG monoclonal anti-mouse F4/80 (Clone Cl:A3-1; Abcam; Dilution 1:50) or rat IgG monoclonal anti-mouse Endomucin (Clone V.7C/.1; Abcam; Dilution 1:50). The day after, sections were washed in PBS and incubated with goat anti-rat IgG, horseradish peroxidase conjugated antibody (GE Healthcare; Dilution 1:100) in wash solution for 1 hour in a humid chamber at RT. Development was performed with DAB (3,3-diaminobenzidine) labeling system (Vector Laboratories, Burlingame, CA). Sections were then counterstained with Gill's hematoxylin for 2 minutes, dehydrated using graded alcohols (75%, 96% and 100%) and xylene, and mounted with DPX (Sigma). Negative controls were generated on adjacent sections by omitting the primary antibodies.

Statistics

The results are presented as mean ± SD, and the statistical differences between 2 groups were determined by the unpaired Student *t*-test or for multiple group comparisons, the one-way ANOVA test with a Tukey's posttest was performed using GraphPad Prism software (San Diego, CA, USA). Statistically significant is labeled * for $P<0.05$, ** for $P<0.01$ and *** for $P<0.001$ or + for $P<0.05$, ++ for $P<0.01$ and +++ for $P<0.001$.

RESULTS

Necrosis occurs in macroscopic visible granulomas in C57BL/6 mice

As referred previously, the Appelberg group has developed a study model using C57BL/6 mice infected with a low dose inoculum of a virulent strain of *M. avium* (ATCC 25291) [69, 82]. This study model allowed the establishment of a progressive infection characterized by the formation of small granulomas which gradually increased in size to macroscopic lesions and evolved to central necrosis at four months post-infection as it is shown in figure 6. Liver macroscopic analysis from infected C57BL/6 mice revealed lesion sizes between 1 and 3 mm in diameter (Fig. 6D). The hypothesis formulated in this work was that granuloma necrosis could take place when the inflammatory lesions reached larger sizes, generating a hypoxic environment leading to necrosis.

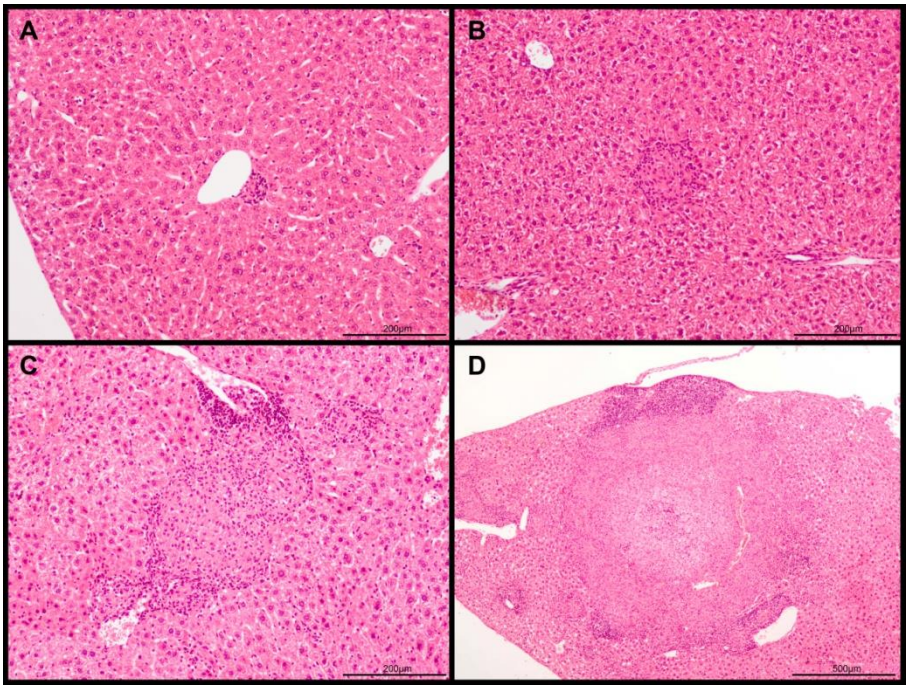

Figure 6 - Granuloma progression in the livers from C57BL/6 mice infected with *M. avium* 25291. Representative lesions in HE stained liver sections from animals intravenously infected with 100 CFUs of *M. avium* 25291, at days 30 (A), 60 (B), 90 (C) and 120 (D) post-infection.

Granuloma vascularization during granuloma progression in C57BL/6 mice

The role of nutrient deprivation and hypoxia in the granuloma necrosis has been described. In fact, granulomas are poorly vascularized structures which lead to a diminished

blood supply and consequently to a reduction of nutrient and oxygen at the central core [87]. To evaluate vascularization during granuloma development we evaluated the expression of endomucin, a known endothelial cell marker [124], by immunohistochemistry (IHC). A positive staining was observed on the capillaries surrounding small granulomas, inside the intermediate size granuloma and in areas immediately surrounding the necrotic core of bigger granulomas (Fig. 7 A-C). No staining was observed in necrotic areas of intermediate size granuloma (Fig. 7D) or in the center of necrotic granuloma since it consisted of amorphous acellular content.

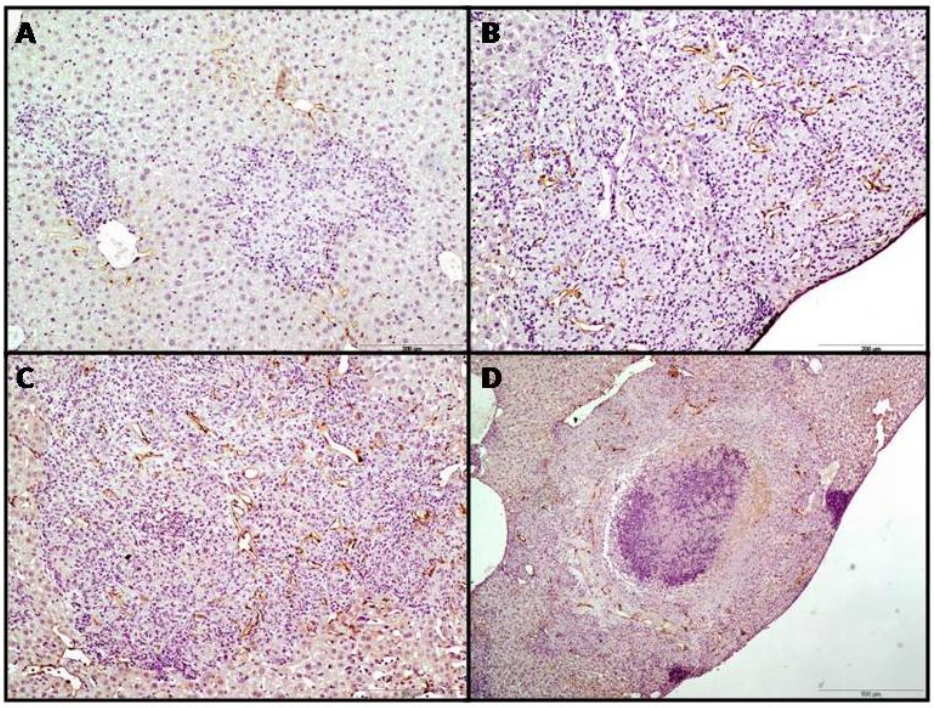

Figure 7 - Endomucin expression evaluation in the livers from C57BL/6 mice infected with *M. avium* 25291. Paraffin sections of livers were analyzed by IHC using mAb endomucin (A – D). Endomucin expression was evaluated at days 90 (A) and 120 (B – D) post-infection.

Granulomata is mainly constituted by macrophages

Some studies have been focused on the role of macrophages under hypoxic conditions. It has been described that under hypoxic conditions myeloid cell properties such as transmigration, motility and invasion could be affected [109]. In this work, we evaluated the granuloma constitution on macrophages using F4/80, a known cell marker for resident (Kupffer cells) and recruited macrophages [125]. The F4/80 expression was evaluated by IHC, using liver histological sections from infected C57BL/6 mice (Fig. 8 A-D). The results showed a positive staining in the granulomas from day 30 until 120 post-infection, indicating that

macrophages are present in small granulomas as well as in bigger granuloma, which were shown to be poorly vascularized.

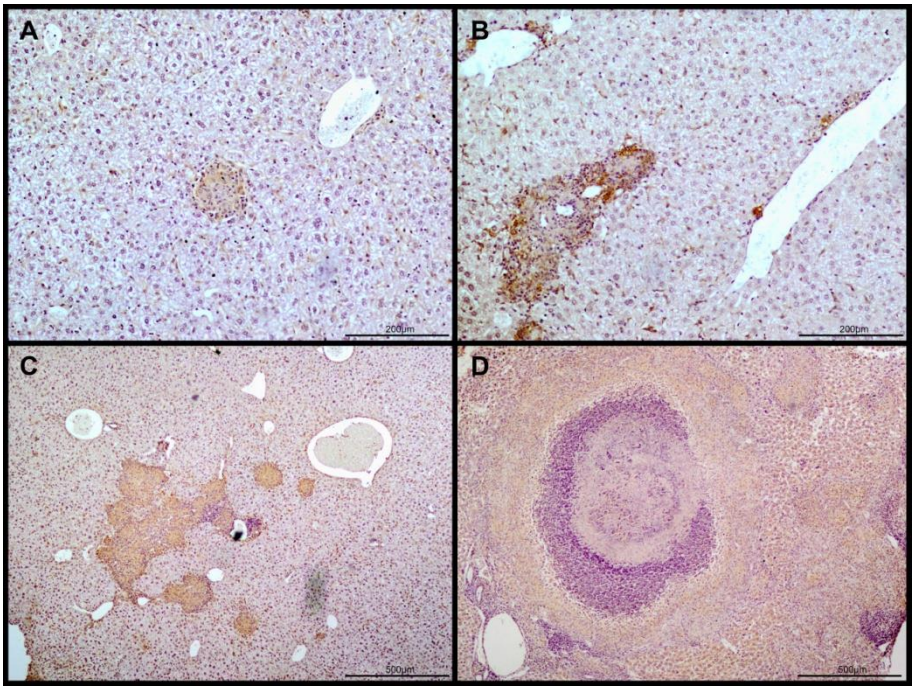

Figure 8 – F4/80 expression evaluation in the livers from C57BL/6 mice infected with *M. avium* 25291. Paraffin sections of livers were analyzed by IHC using mAb F4/80 (A - D). F4/80 expression was evaluated at days 30 (A), 60 (B), 90 (C) and 120 (D) post-infection.

HIF-1α is increased during *M. avium* infection

Previous studies have shown the presence of hypoxic regions at the center of necrotic granulomas induced by *M. tuberculosis* or *M. avium* infection [85-87]. Furthermore, since our observations revealed that small non-necrotic granulomas were poorly vascularized structures, and as the granulomas enlarged, the central core became less vascularized, probably leading to a decrease in oxygen supply, constituting an hypoxic environment, we hypothesized that hypoxia could be the major cause for granuloma necrosis in our study model. Therefore and considering HIF-1α to be the master regulator of hypoxia [91, 97], we evaluated HIF-1α protein content in liver mononuclear cells during *M. avium* infection. A significant increase of total HIF-1α protein levels in the liver mononuclear cells from infected animals was found compared with the non-infected animals, starting at day 60 post-infection (Fig. 9). These results indicate a HIF-1α accumulation, before the onset of granuloma necrosis (60 days and 90 days post-infection).

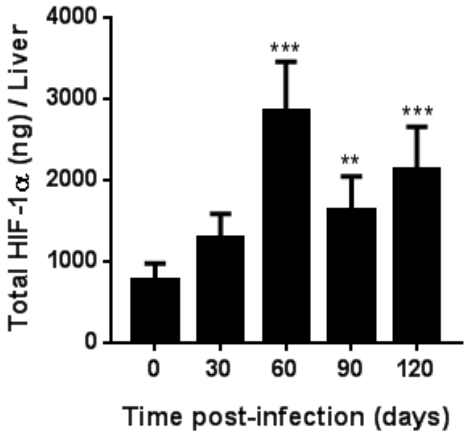

Figure 9 - Analysis of total HIF-1α protein in liver mononuclear cells during *M. avium* infection. C57BL/6 mice were intravenously infected with 100 CFUs of *M. avium* 25291. Total HIF-1α protein was determined at days 0, 30, 60, 90 and 120 post-infection by ELISA as described in the material and methods section. Groups of non-infected mice (day 0) were included at every time-point of infection studied. Each group of non-infected mice comprised three to four animals and each group of infected mice comprised four to six animals. Data are expressed as means ± S.D. of protein levels calculated to the total liver mononuclear cells for individual mice. ** $P<0.01$, *** $P<0.001$ using unpaired student *t*-test, comparing values from infected and non-infected animals.

HIF-1α absence leads to higher bacterial load

In order to determine the relevance of HIF-1α in *in vivo* on the proliferation of *M. avium*, WT and HIF-1α$^{-/-}$ mice were infected with 100 CFUs of *M. avium* 25291, and the bacterial loads were quantified in the liver and spleen at different time-points of infection. As shown in figure 10, the infection of both strains of mice resulted in a progressive infection with no evidence of bacterial control as previously described [69]. The growth patterns of bacteria in the spleen and liver from infected mice were in agreement with previous observations [69]. HIF-1α$^{-/-}$ mice showed increased bacterial loads within the spleen starting at day 15 post-infection compared to WT mice (Fig. 10B). Concerning the liver, an increased bacterial load was found in HIF-1α$^{-/-}$ mice compared to WT mice only at days 15 and 104 (Fig. 10A). The results indicate that presence of HIF-1α is important in the control of *M. avium* infection as suggested in other infection models [111, 126]. Therefore, it might be hypothesized that the exacerbation of infection occurs probably due to the lack of hypoxia adaptation mechanisms.

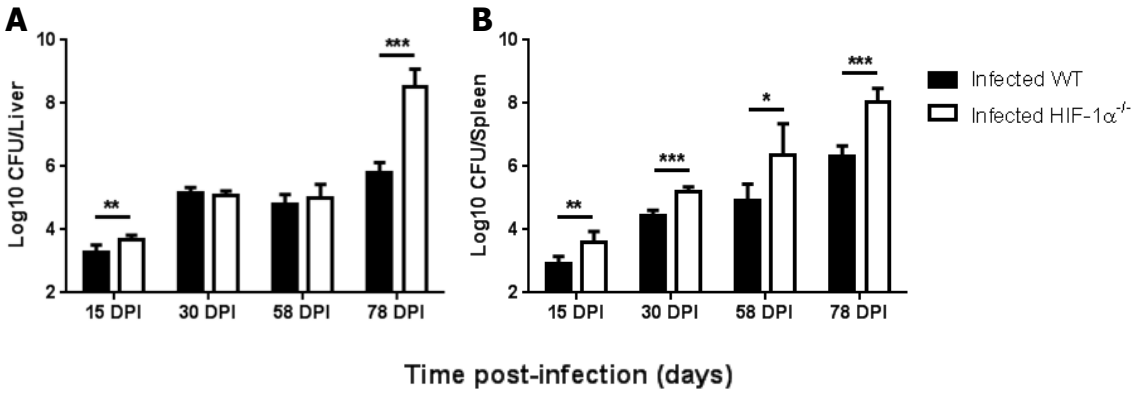

Figure 10 – HIF-1α presence is important in the control of *M. avium* infection. Growth of *M. avium* 25291 in liver and spleen from WT and HIF-1α$^{-/-}$ mice intravenously infected with 100 CFUs. Bacterial load was determined at different time points (15, 30, 60 and 78 days post-infection). Each time-point represents the mean of the $\log_{10}$ CFUs per organ ± SD from at least five mice per group.* $P<0.05$, ** $P<0.01$, *** $P<0.001$ using unpaired student *t*-test.

HIF-1α deficient mice develop necrotic granulomas earlier compared with C57BL/6 mice

In order to understand the involvement of HIF-1α during *M. avium* infection, we used a mouse model with a genetic ablation of the HIF-1α transcription factor in the myeloid lineage (monocytes, mature macrophages, and granulocytes). In a first attempt to determine the influence of HIF-1α deficiency, we analyzed the granuloma progression during infection in HIF-1α$^{-/-}$ and WT mice by histological analysis. HIF-1α$^{-/-}$ and WT mice were intravenously infected with 100 CFUs of *M. avium* 25291 and were euthanized at different time-points post-infection. Previous observations indicated that in WT mice, the granuloma central necrosis started around four months post-infection (Fig. 6D). In the beginning of the infection lesions in both HIF-1α$^{-/-}$ and WT mice were very small and incipient (Fig. 11A, 11D). By day 60 post-infection, well-structured granulomas were found with an extensive lymphoid cuff surrounding the macrophage core in WT mice (Fig. 11B) as previously reported [69]. By day 104 post-infection, many of those granulomas were found with additional extensive lesions consisting of peripheral accumulations of lymphoid cells, fibrosis and vascularization (Fig. 11C). As show in Figure 11 (A – F), after day 60 post-infection, differences were evident between the lesions in both strains of mice. In fact, in the absence of HIF-1α the onset of necrosis was faster compared with WT mice. After day 78 post-infection (data not shown), macroscopically visible tubercles were present in HIF-1α$^{-/-}$ mice. Central necrosis was observed in all the HIF-1α$^{-/-}$ mice analyzed at days 78 and 104 post-infection. Microscopically, these lesions

exhibited a well-defined necrotic core with infected macrophages, surrounded by a fibrotic capsule and accumulations of lymphoid cells as described previously (Fig. 11 F-I). In contrast, caseation was not observed in any of the WT animals analyzed at days 78 and 104 post-infection. Morphometric analysis determining the infiltrated necrotic or non-necrotic area, confirmed the role of HIF-1α on the granuloma progression. Thus, a statistically significant increase of necrotic and non-necrotic areas was found in HIF-1α$^{-/-}$ compared with WT mice at day 104 post-infection (Fig. 11G). No differences were found at day 30 post-infection. At day 60 post-infection, despite the slight increase of the non-necrotic area in HIF-1α$^{-/-}$ compared with WT mice, no statistically significant difference was observed. Similarly, a high number of cellular infiltrates were observed in HIF-1α$^{-/-}$ compared with WT mice at day 104 post-infection (Fig. 11H). No statistically significant differences were observed in the number of cellular infiltrates (Fig. 11H) at day 30 or 60 post-infection. These results indicate that absence of HIF-1α in myeloid cells anticipates the granuloma necrosis and increases the inflammatory cell infiltration during *M. avium* infection.

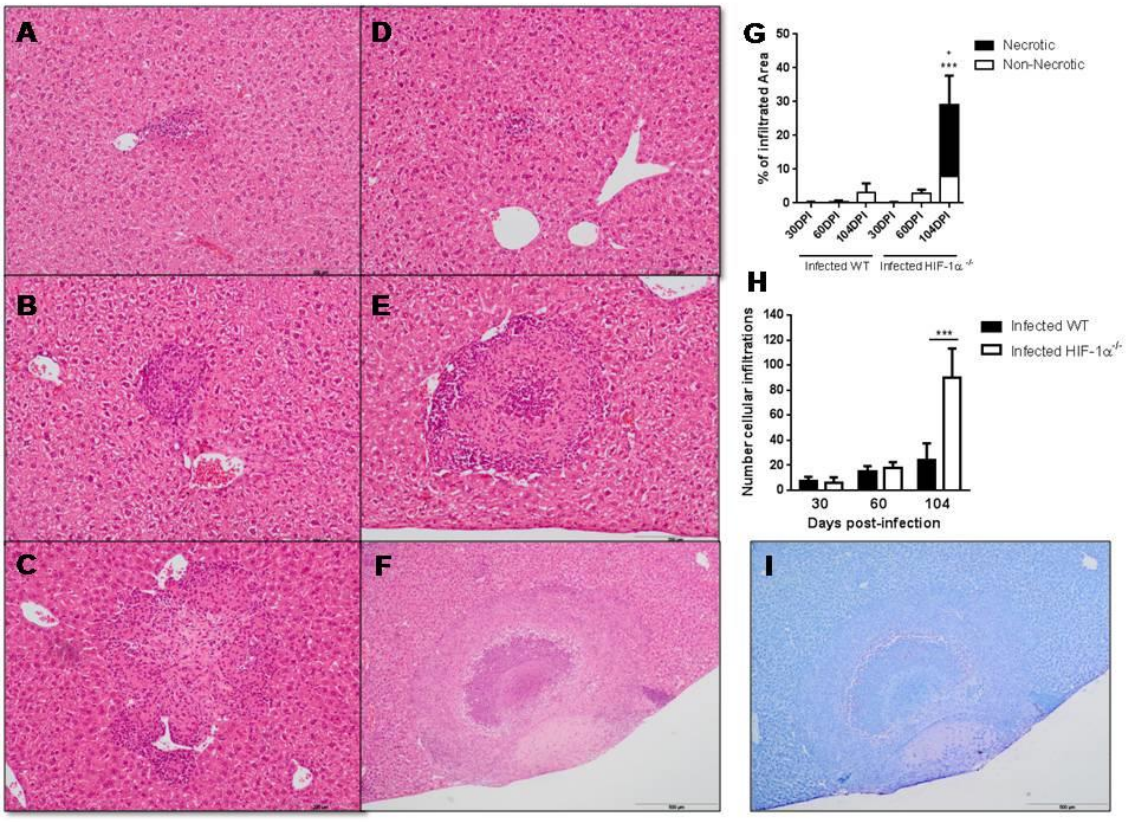

Figure 11 – HIF-1α absence influences granuloma progression during *M. avium* infection. Representative lesions in HE (A-F) or Ziehl-Neelson (I) stained liver sections from WT (A-C) and HIF-1α$^{-/-}$ (D-F and I) intravenously infected with 100 CFUs of *M. avium* 25291 at days 30 (A, D), 60 (B, E), and 104 (C, F, I) post-infection. (I) provides a higher power view to show an intermediate layer of heavily infected macrophages and an inner core with necrotic material. The percentage of infiltrating

area (G) and the number of cellular infiltrates (H) were determined as described in the material and methods section. Data are expressed as mean ± S.D of the areas from mice analyzed individually in each group. *** $P<0.001$ using unpaired student *t*-test to compare infected and non-infected. $^{+}P<0.05$ using unpaired student *t*-test to compare the area of necrotic *versus* non-necrotic.

HIF-1α absence induces splenomegaly and hepatomegaly during *M. avium* infection

Representative photographs of spleens and livers from infected WT or HIF-1α$^{-/-}$ mice at day 96 post-infection are shown in figure 12. Infected HIF-1α$^{-/-}$ exhibited a extensive splenomegaly and hepatomegaly, when compared with the infected WT. Macroscopic observation of the spleens and livers from non-infected WT or HIF-1α$^{-/-}$ animals indicated no differences (data not shown). A slight splenomegaly and hepatomegaly was evident between the infected WT and the non-infected WT (data not shown). Furthermore, the observation of livers from infected WT and HIF-1α$^{-/-}$ animals, showed the presence of necrotic granulomas at day 96 post-infection. These observations indicate that HIF-1α influenced the size and probably the cellularity of the spleen and livers from mice infected with *M. avium* 25291.

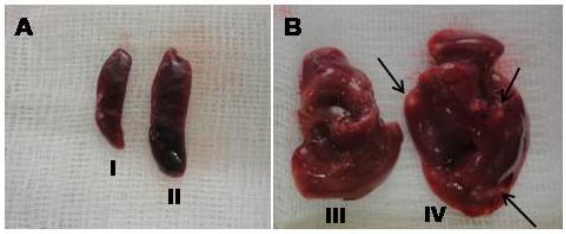

Figure 12 – HiF-1α absence induces an increase of spleen and liver sizes during infection with *M. avium* 25291. Photographs of livers from WT and HIF-1α$^{-/-}$ mice infected with 100 CFU *M. avium* 25291 at day 96 post-infection. Representative images of spleens (A) and livers (B) from WT (I and III) and HIF-1α$^{-/-}$ (II and IV) mice.

Infected HIF-1α deficient mice present increased cellularity

Macroscopic observation of the livers and spleens from *M. avium* infected HIF-1α$^{-/-}$ mice indicated an increase in the size and suggested a probable increase in the cellularity in these organs. It was previously shown that normal numbers of T cells and macrophages persisted after day 60 post-infection when using WT mice infected with a low dose of *M. avium* 25291 [69]. In order to determine the requirement of a given cell population in the earlier development of necrosis in HIF-1α$^{-/-}$ mice, we decided to analyze the spleen and liver mononuclear cells by flow cytometry from control or infected WT and HIF-1α$^{-/-}$ mice (Fig. 13).

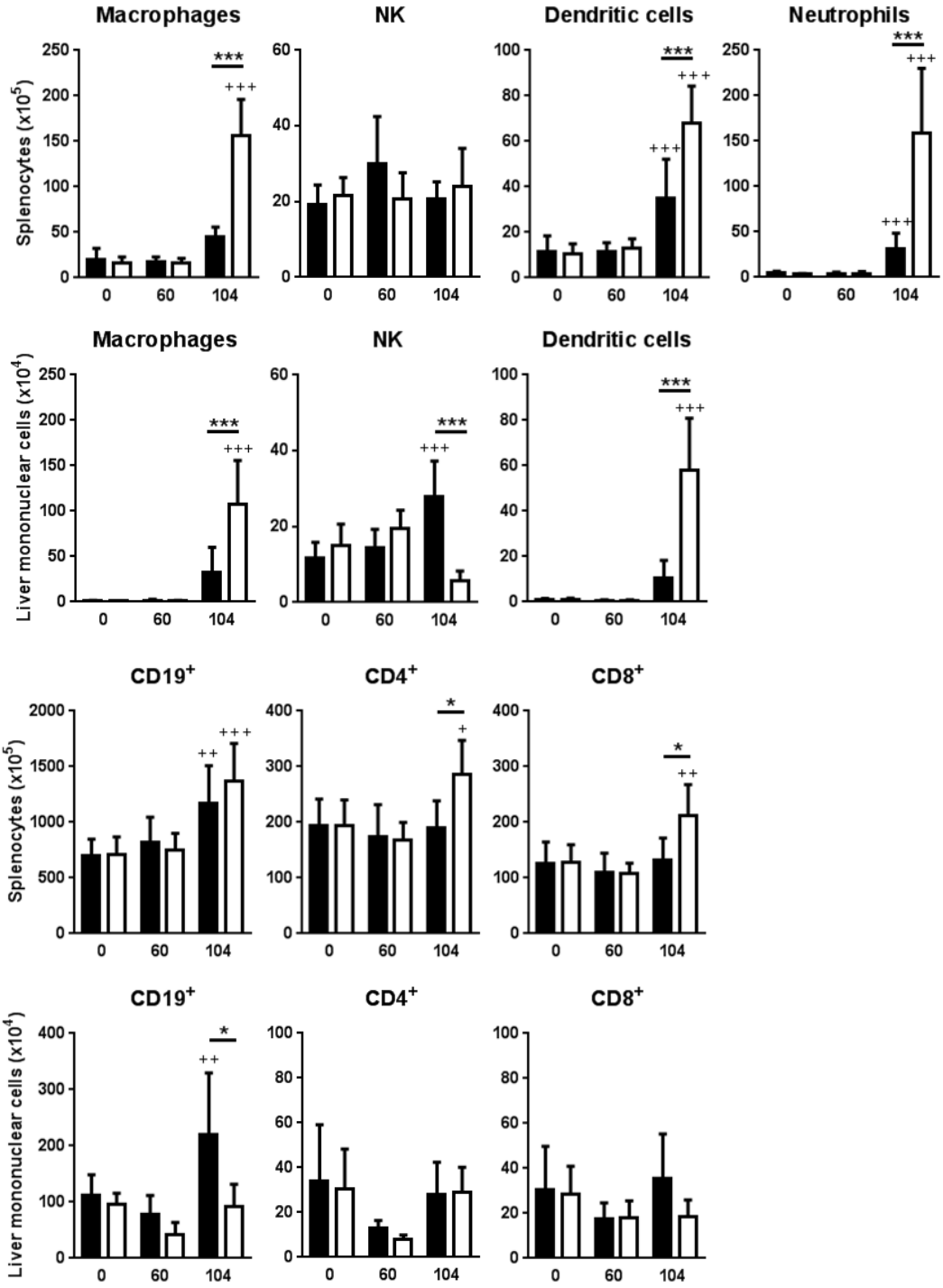

Figure 13 – *M. avium* infected HIF-1α deficient mice present increased cellularity. Cellular composition of the spleens (A) and livers (B) from WT and HIF-1α$^{-/-}$ mice infected with 100 CFU of *M. avium* 25291 at different time points post-infection. Each group comprised at least 5 animals. All data are expressed as means + SD. **P*<0.05, ***P*<0.01, *** *P*<0.001 using unpaired student *t*-test, comparing infected groups within the same time point. ^{+}P<0.05, ^{++}P<0.01, ^{+++}P<0.001 using unpaired student *t*-test, comparing infected *versus* non-infected animals.

The analysis of the spleen showed a significant increase in the number of DCs and neutrophils at day 104 post-infection in both infected WT and HIF-1α$^{-/-}$ mice, compared to non-infected WT and HIF-1α$^{-/-}$, respectively. In accordance with the evident splenomegaly observed in infected HIF-1α$^{-/-}$ mice, a significant increase in the numbers of macrophages, DCs and neutrophils was found compared with infected WT mice. In addition, the analysis of the liver mononuclear cells revealed a significant increase in the number of macrophages and DCs from infected HIF-1α$^{-/-}$ mice, compared to infected WT mice. The analysis of the spleen lymphocyte population did not shown any differences between the infected and non-infected groups in the beginning of infection, as previously was shown [69]. At day 104 post-infection, a significant increase in all spleen lymphocyte population was noticed, which is in agreement with the evident splenomegaly observed in infected HIF-1α$^{-/-}$ mice. In contrast, no differences were observed in the analysis of liver lymphocyte populations, with the exception of CD19^{+} cells. Curiously a significant increase of CD19^{+} cells in the liver was observed in infected WT compared to HIF-1α$^{-/-}$ mice, suggesting a higher recruitment of B cells in the presence of HIF-1α presence.

DISCUSSION

In the past few years many cellular and molecular mechanisms underlying the structuring of granuloma have been described. However, the mechanism that leads to necrosis still poorly understood. Previous work has shown that this process is highly dependent on $CD4^+$ T cells, IFNγ and IL-12, and partly on IL-6 and CD40 [69, 127]. In fact, *M. avium* intravenously infected mice lacking CD4 T cells, IFN-γ, IL-12, IL-6 and the co-stimulatory molecule CD40 failed to develop granuloma necrosis [69]. Additionally, the infection of DBA/1 strain [82] also failed to induce macroscopic lesions and did not develop to necrosis [69]. In contrast, it was possible to find macroscopic lesions undergoing necrosis in C57BL/6 mice lacking TNF-α [75], NO or $CD8^+$ T cells [69]. Thus, in the beginning of this work, we hypothesized that the granuloma size could be a crucial factor in the development of necrosis during *M. avium* infection. As suggested by Orme, necrosis did not occur when the T cells reached the center of the granulomas. In contrast, local necrosis occurred either in fibrotic granulomatous lesions or when T cells remained at the peripheral mantle not invading the center of the lesion [128]. The data obtained in our work suggest that the absence of lymphocytes at the center of granuloma is a possible consequence of the reduced vascularization in the center of the granuloma. Recently, it has been described that necrotic granulomas developed in *M. tuberculosis*-infected guinea pigs, rabbits and nonhuman primates [85], and also in *M. avium* strain TMC724-infected C57BL/6 mice were hypoxic [87]. In our study, we used C57BL/6 mice infected with *M. avium* 25291 to address the granuloma vascularization during granuloma progression. The absence of vascularization in small granulomas, and the vascularization of large granulomas without necrosis, probably occurred due to a homeostatic process of angiogenesis in an attempt to prevent a hypoxic environment in the granuloma. Curiously, no vascularization was observed in the center of bigger lesions, just before they become necrotic. Our observations are in agreement with other studies, also in the context of *M. avium* infection, where a decreased vascularization in the central areas of the granuloma was demonstrated [129]. Having in mind these results, we can argue that the center of larger granulomas becomes less vascularized, resulting in a hypoxic environment that will lead to necrosis in the center of granuloma. To better define a possible role of hypoxia in the development of necrotic granulomas in our study model, we decided to assess the influence of HIF-1α. In the last 20 years, HIF-1α has been described as the master regulator of physiological and cellular mechanisms indispensable in the adaptation to hypoxia [97, 106, 109]. Under hypoxic conditions, the levels of HIF-1α increase by accumulation [97, 109]. In our study model, we found an increase in the total HIF-1α protein in liver mononuclear cells during infection. Curiously, the peak of HIF-1α production occurred 60 days after infection, which corroborates the observation of a reduced vascularization of the granulomas before the beginning of necrosis development. Based on this, it is possible to postulate that granulomas became hypoxic before the onset of granuloma necrosis.

However, another alternative explanation may justify the increase of HIF-1α in early time points of *M. avium* infection. Recently, it has been proposed that other factors, rather than only hypoxia, are able to modulate HIF-1α expression and degradation. In fact, even under normoxia, HIF-1α is induced by bacterial infection and regulated by TNFα and IFNγ [93, 111, 121, 122]. Tissue macrophages are believed to play an important role in the resistance against mycobacteria infection being its recruitment and activation crucial in the control of bacteria proliferation [6, 7] . It has been described that 95% of the activated macrophages present in inflammation infiltrates are derived from exudate monocytes [108], and that they need to move against oxygen gradients in order to migrate toward the areas of inflammation [106, 130]. Our results show macrophage accumulation within the infection site even in late time-points of infection, where hypoxic conditions may occur. This is in accordance with other studies, indicating that infiltrating macrophages are able to adapt to low oxygen conditions [106, 130]. Cramer *et al* has described using *in vitro* assays and Group B *Streptococcus* infection of macrophages, a significant impairment of motility and invasion of HIF-1α deficient macrophages, with a 7-fold increase of bacterial load in the absence of HIF-1α [109]. In our study, the qualitatively analysis of F4/80 expression in the liver sections from infected WT and HIF-1α deficient mice did not indicate any differences in the accumulation of macrophages (data not shown). It was found that at early stages of infection, HIF-1α deficient mice failed to restrict the spread of the bacteria. This clearly shows that bacterial killing is limited in the absence of HIF-1α. The exacerbation of infection in HIF-1α deficient mice probably occurred due to the (i) failure in controlling bacterial growth caused by the absence of hypoxia adaptation mechanisms and (ii) different levels of IFNγ production in the HIF-1α absence. We could argue that the differences in bacterial numbers between WT and HIF-1α deficient mice could be due to low levels of IFNγ in the absence of HIF-1α. In fact, it has been previously shown, that IFNγ is involved in early and later protection against *M. avium infection* [38, 39]. However, in our study, we did not observe significant differences in the production of IFNγ during infection in WT compared to HIF-1α deficient mice (data not shown). These results suggested that the differences in the bacterial numbers between WT and HIF-1α deficient mice were due to different levels of IFNγ production. Therefore, we hypothesize that exacerbation of infection in HIF-1α deficient mice mostly occurs in response to a failure in the control of bacterial growth caused by an interference of hypoxia adaptation mechanisms. The splenomegaly and hepatomegaly developed at latter time-points of *M. avium* infection reflect the increased recruitment of different types of immune cells respectively to the spleen and liver. In fact, a statistically significant increase in cell numbers from myeloid cell lineage, namely macrophages, neutrophils and DCs was found in infected HIF-1α deficient mice compared to WT mice, but that were not correlated with a better protection against *M. avium* infection. These observations are coincident with granuloma

necrosis occurrence in infected HIF-1α deficient mice but not in WT mice. This probably occurs due to an emergence of the immune system in response to inflammation. The granuloma disintegration leads to the release of virulent bacteria from dead macrophages, allowing bacteria to disseminate in the tissue spreading and infecting other tissues [6]. Concerning the analysis of lymphocytes, a significant increase in the numbers of spleen T cells from infected HIF-1α deficient mice was found comparing to WT mice at later time-points of infection. No differences were observed in the liver. Flórido *et al* have described, using *M. avium* aerosol infection of TNF deficient mice, the development of pulmonary granuloma disintegration that led to an extensive expansion of T cells and macrophages [55]. It seems therefore, that besides T cells, also macrophages, DCs and neutrophils are determinant in the disintegration of the granuloma occurring in the liver in our study model. The Appelberg group has described a model of mycobacterial infection featuring the development of lesions containing causeous necrotic material. Additionally, the development of necrosis in this model required an intact type 1 immune axis [69]. Interestingly, the phenotype resulting from the loss of HIF-1α in the myeloid cell lineage showed clear differences between WT and HIF-1α deficient mice. The results obtained in this work are consistent with previous findings showing that, WT mice intravenously infected with 100 CFUs of *M. avium* 25291, developed granuloma with central necrosis after four months of infection [69]. The morphometric analysis of liver sections at days 30 and 60 post-infection has shown small, but not significant differences, in the numbers of cellular infiltrates and in the percentage of infiltrated area in WT and HIF-1α deficient mice. Keeping in mind these results, the analysis of spleen or liver cellularity in generally showed equal numbers at earlier time-points of infection. In contrast, the bacterial numbers were significantly increased in HIF-1α deficient mice compared to WT mice at these time-points of infection. In summary, at early stages of infection, the differences in bacterial burdens are not reflected either in cellularity or in the infiltrating area. Theoretically, the increase observed in the intracellular bacterial loads in the absence of HIF-1α at late stages of infection should reflect an accelerated necrotic death of infected macrophages in the granuloma and bacteria tissue dissemination [109, 131]. This assumption was confirmed, since, the absence of HIF-1α led to an increase of cellular infiltrates, an increase of granuloma size and consequently an anticipation of necrosis. The increased size of granuloma suggests that augmented bacterial load led to increased numbers of heavily infected macrophages and other immune cells types. The lack of hypoxia adaptation mechanisms in macrophages leads to evident differences in the progression of *M. avium* infection. Here we provide evidence that HIF-1α plays a crucial role in the development of necrosis in this type of immunopathology.

In conclusion, the work presented here gives a plausible explanation regarding the development of necrotic granulomas during *M. avium* infection. Altogether, we provide

evidences suggesting that granulomas are hypoxic before underging necrosis, through the analysis of vascularization and quantification of HIF-1α in a necrotizing mice model. Further, we used a mice model with a genetic ablation of the HIF-1α transcription factor in the myeloid lineage which clearly induces an impairment of the resistance against *M. avium* infection. All these data together show that hypoxia is one of the major causes in the progression to necrosis. This work indicates that by the manipulation or modulation of macrophage hypoxic adaptation during infection it might be possible to avoid pathology.

Future perspectives

The present work has shown that exacerbation of the *M. avium* infection and the onset of necrosis is a direct consequence of the lack of HIF-1α in myeloid cells. It has been also clear that macrophages adaptation to hypoxic conditions is crucial to the resistance against *M. avium* infection. To confirm this observation, we could perform *in vitro* studies using macrophages from a WT and HIF-1α deficient mice exposed to *M. avium* to quantified the bacterial load in both normoxia and hypoxia conditions. The activation of macrophages by IFNγ is a crucial step in the resistance against *M. avium* infection and different levels of IFNγ can lead to a profound impact in the activation of macrophages and consequently in the bacterial burdens. Since the macrophage activation is IFNγ-dependent, it is important to understand the role of IFNγ during the *M. avium* infection. During this work we only have observed the IFNγ production in later stages of the infection, since the necrosis occurs in late time-points of infection, however, we could perform an assay to quantify IFNγ in early time points of infection.

Here we hypothesized that appearance of hypoxic regions at the center of granuloma occurs before the development of necrosis in *M. avium* infection. The appearance of hypoxic regions induces a cellular adaptation mechanism which is a HIF-1α-dependent process. Since the results showed an exacerbation of *M. avium* numbers in the absence of HIF-1α in myeloid cells, it would be interesting trying to control the bacterial burdens, using mice with HIF-1α over expressed. The lack of vascularization in the center of granuloma seems to be a crucial step in the development of necrosis either in WT or HIF-1α deficient mice. This process is mainly regulated by angiogenesis factors, namely VEGF. We could use mice with VEGF over expressed in order to try to increase the ability to re-vascularize and re-oxygenate the center of the granuloma and consequently prevent the development of necrosis. On the other hand, we could use knockout mice for VEGF, which will probably

exacerbate the *M. avium* infection despite the ability of hypoxic adaptation in macrophages are intact.

REFERENCES

1. Organization WH. Global tuberculosis report 2014. Geneva: World Heath Organization, 2014.
2. Murray JF. Mycobacterium tuberculosis and the cause of consumption: from discovery to fact. Am J Respir Crit Care Med 2004; 169:1086-8.
3. Daniel TM. The history of tuberculosis. Respir Med 2006; 100:1862-70.
4. Organization WH. WHO: Tuberculosis - Global Facts 2011/2012. Geneva: WHO - Stop TB Department, 2012.
5. Glaziou P, Falzon D, Floyd K, Raviglione M. Global epidemiology of tuberculosis. Semin Respir Crit Care Med 2013; 34:3-16.
6. O'Garra A, Redford PS, McNab FW, Bloom CI, Wilkinson RJ, Berry MP. The immune response in tuberculosis. Annu Rev Immunol 2013; 31:475-527.
7. Flynn JL, Chan J. Immunology of tuberculosis. Annu Rev Immunol 2001; 19:93-129.
8. Wang J, Behr MA. Building a better bacillus: the emergence of Mycobacterium tuberculosis. Front Microbiol 2014; 5:139.
9. Cosma CL, Sherman DR, Ramakrishnan L. The secret lives of the pathogenic mycobacteria. Annu Rev Microbiol 2003; 57:641-76.
10. Tortoli E. The new mycobacteria: an update. FEMS Immunol Med Microbiol 2006; 48:159-78.
11. Johnson MM, Odell JA. Nontuberculous mycobacterial pulmonary infections. J Thorac Dis 2014; 6:210-20.
12. Cook JL. Nontuberculous mycobacteria: opportunistic environmental pathogens for predisposed hosts. Br Med Bull 2010; 96:45-59.
13. Corti M, Palmero D. Mycobacterium avium complex infection in HIV/AIDS patients. Expert Rev Anti Infect Ther 2008; 6:351-63.
14. Karakousis PC, Moore RD, Chaisson RE. Mycobacterium avium complex in patients with HIV infection in the era of highly active antiretroviral therapy. Lancet Infect Dis 2004; 4:557-65.
15. Russell DG, Cardona PJ, Kim MJ, Allain S, Altare F. Foamy macrophages and the progression of the human tuberculosis granuloma. Nat Immunol 2009; 10:943-8.
16. Gengenbacher M, Kaufmann SH. Mycobacterium tuberculosis: success through dormancy. FEMS Microbiol Rev 2012; 36:514-32.
17. Takeda K, Kaisho T, Akira S. Toll-like receptors. Annu Rev Immunol 2003; 21:335-76.
18. Shi Z, Cai Z, Sanchez A, Zhang T, Wen S, Wang J, et al. A novel Toll-like receptor that recognizes vesicular stomatitis virus. J Biol Chem 2011; 286:4517-24.
19. Underhill DM, Ozinsky A, Hajjar AM, Stevens A, Wilson CB, Bassetti M, et al. The Toll-like receptor 2 is recruited to macrophage phagosomes and discriminates between pathogens. Nature 1999; 401:811-5.
20. Wang T, Lafuse WP, Zwilling BS. Regulation of toll-like receptor 2 expression by macrophages following Mycobacterium avium infection. J Immunol 2000; 165:6308-13.
21. Gomes MS, Flórido M, Cordeiro JV, Teixeira CM, Takeuchi O, Akira S, et al. Limited role of the Toll-like receptor-2 in resistance to Mycobacterium avium. Immunology 2004; 111:179-85.
22. Feng CG, Scanga CA, Collazo-Custodio CM, Cheever AW, Hieny S, Caspar P, et al. Mice lacking myeloid differentiation factor 88 display profound defects in host resistance and immune responses to Mycobacterium avium infection not exhibited by Toll-like receptor 2 (TLR2)- and TLR4-deficient animals. J Immunol 2003; 171:4758-64.
23. Appelberg R. Pathogenesis of Mycobacterium avium infection: typical responses to an atypical mycobacterium? Immunol Res 2006; 35:179-90.
24. Russell DG, Mwandumba HC, Rhoades EE. Mycobacterium and the coat of many lipids. J Cell Biol 2002; 158:421-6.

25. Oh YK, Straubinger RM. Intracellular fate of Mycobacterium avium: use of dual-label spectrofluorometry to investigate the influence of bacterial viability and opsonization on phagosomal pH and phagosome-lysosome interaction. Infect Immun 1996; 64:319-25.
26. Fuchs R, Schmid S, Mellman I. A possible role for Na+,K+-ATPase in regulating ATP-dependent endosome acidification. Proc Natl Acad Sci U S A 1989; 86:539-43.
27. Russell DG, Vanderven BC, Glennie S, Mwandumba H, Heyderman RS. The macrophage marches on its phagosome: dynamic assays of phagosome function. Nat Rev Immunol 2009; 9:594-600.
28. Clemens DL, Horwitz MA. Characterization of the Mycobacterium tuberculosis phagosome and evidence that phagosomal maturation is inhibited. J Exp Med 1995; 181:257-70.
29. Armstrong JA, Hart PD. Response of cultured macrophages to Mycobacterium tuberculosis, with observations on fusion of lysosomes with phagosomes. J Exp Med 1971; 134:713-40.
30. Crowle AJ, Dahl R, Ross E, May MH. Evidence that vesicles containing living, virulent Mycobacterium tuberculosis or Mycobacterium avium in cultured human macrophages are not acidic. Infect Immun 1991; 59:1823-31.
31. Rook GA, Champion BR, Steele J, Varey AM, Stanford JL. I-A restricted activation by T cell lines of anti-tuberculosis activity in murine macrophages. Clin Exp Immunol 1985; 59:414-20.
32. Appelberg R, Sarmento AM. The role of macrophage activation and of Bcg-encoded macrophage function(s) in the control of Mycobacterium avium infection in mice. Clin Exp Immunol 1990; 80:324-31.
33. Rohde K, Yates RM, Purdy GE, Russell DG. Mycobacterium tuberculosis and the environment within the phagosome. Immunol Rev 2007; 219:37-54.
34. Hussain S, Zwilling BS, Lafuse WP. Mycobacterium avium infection of mouse macrophages inhibits IFN-gamma Janus kinase-STAT signaling and gene induction by down-regulation of the IFN-gamma receptor. J Immunol 1999; 163:2041-8.
35. Petrofsky M, Bermudez LE. CD4+ T cells but Not CD8+ or gammadelta+ lymphocytes are required for host protection against Mycobacterium avium infection and dissemination through the intestinal route. Infect Immun 2005; 73:2621-7.
36. Schaible UE, Sturgill-Koszycki S, Schlesinger PH, Russell DG. Cytokine activation leads to acidification and increases maturation of Mycobacterium avium-containing phagosomes in murine macrophages. J Immunol 1998; 160:1290-6.
37. Rhoades ER, Ullrich HJ. How to establish a lasting relationship with your host: lessons learned from Mycobacterium spp. Immunol Cell Biol 2000; 78:301-10.
38. Appelberg R, Castro AG, Pedrosa J, Silva RA, Orme IM, Minóprio P. Role of gamma interferon and tumor necrosis factor alpha during T-cell-independent and -dependent phases of Mycobacterium avium infection. Infect Immun 1994; 62:3962-71.
39. Saunders BM, Cheers C. Inflammatory response following intranasal infection with Mycobacterium avium complex: role of T-cell subsets and gamma interferon. Infect Immun 1995; 63:2282-7.
40. Gomes MS, Appelberg R. NRAMP1- or cytokine-induced bacteriostasis of Mycobacterium avium by mouse macrophages is independent of the respiratory burst. Microbiology 2002; 148:3155-60.
41. Segal BH, Doherty TM, Wynn TA, Cheever AW, Sher A, Holland SM. The p47(phox-/-) mouse model of chronic granulomatous disease has normal granuloma formation and cytokine responses to Mycobacterium avium and Schistosoma mansoni eggs. Infect Immun 1999; 67:1659-65.
42. Doherty TM, Sher A. Defects in cell-mediated immunity affect chronic, but not innate, resistance of mice to Mycobacterium avium infection. J Immunol 1997; 158:4822-31.

43. Gomes MS, Flórido M, Pais TF, Appelberg R. Improved clearance of Mycobacterium avium upon disruption of the inducible nitric oxide synthase gene. J Immunol 1999; 162:6734-9.
44. Shiloh MU, MacMicking JD, Nicholson S, Brause JE, Potter S, Marino M, et al. Phenotype of mice and macrophages deficient in both phagocyte oxidase and inducible nitric oxide synthase. Immunity 1999; 10:29-38.
45. Forbes JR, Gros P. Divalent-metal transport by NRAMP proteins at the interface of host-pathogen interactions. Trends Microbiol 2001; 9:397-403.
46. Gomes MS, Appelberg R. Evidence for a link between iron metabolism and Nramp1 gene function in innate resistance against Mycobacterium avium. Immunology 1998; 95:165-8.
47. Soe-Lin S, Apte SS, Andriopoulos B, Andrews MC, Schranzhofer M, Kahawita T, et al. Nramp1 promotes efficient macrophage recycling of iron following erythrophagocytosis in vivo. Proc Natl Acad Sci U S A 2009; 106:5960-5.
48. Monack DM, Mueller A, Falkow S. Persistent bacterial infections: the interface of the pathogen and the host immune system. Nat Rev Microbiol 2004; 2:747-65.
49. Medina E, Rogerson BJ, North RJ. The Nramp1 antimicrobial resistance gene segregates independently of resistance to virulent Mycobacterium tuberculosis. Immunology 1996; 88:479-81.
50. Orme IM, Roberts AD, Griffin JP, Abrams JS. Cytokine secretion by CD4 T lymphocytes acquired in response to Mycobacterium tuberculosis infection. J Immunol 1993; 151:518-25.
51. Flórido M, Gonçalves AS, Silva RA, Ehlers S, Cooper AM, Appelberg R. Resistance of virulent Mycobacterium avium to gamma interferon-mediated antimicrobial activity suggests additional signals for induction of mycobacteriostasis. Infect Immun 1999; 67:3610-8.
52. Appelberg R, Orme IM. Effector mechanisms involved in cytokine-mediated bacteriostasis of Mycobacterium avium infections in murine macrophages. Immunology 1993; 80:352-9.
53. Bermudez LE, Young LS. Tumor necrosis factor, alone or in combination with IL-2, but not IFN-gamma, is associated with macrophage killing of Mycobacterium avium complex. J Immunol 1988; 140:3006-13.
54. Appelberg R, Sarmento A, Castro AG. Tumour necrosis factor-alpha (TNF-alpha) in the host resistance to mycobacteria of distinct virulence. Clin Exp Immunol 1995; 101:308-13.
55. Flórido M, Appelberg R. Characterization of the deregulated immune activation occurring at late stages of mycobacterial infection in TNF-deficient mice. J Immunol 2007; 179:7702-8.
56. Hsieh CS, Macatonia SE, Tripp CS, Wolf SF, O'Garra A, Murphy KM. Development of TH1 CD4+ T cells through IL-12 produced by Listeria-induced macrophages. Science 1993; 260:547-9.
57. Seder RA, Gazzinelli R, Sher A, Paul WE. Interleukin 12 acts directly on CD4+ T cells to enhance priming for interferon gamma production and diminishes interleukin 4 inhibition of such priming. Proc Natl Acad Sci U S A 1993; 90:10188-92.
58. Saunders BM, Zhan Y, Cheers C. Endogenous interleukin-12 is involved in resistance of mice to Mycobacterium avium complex infection. Infect Immun 1995; 63:4011-5.
59. Castro AG, Silva RA, Appelberg R. Endogenously produced IL-12 is required for the induction of protective T cells during Mycobacterium avium infections in mice. J Immunol 1995; 155:2013-9.
60. Flórido M, Gonçalves AS, Gomes MS, Appelberg R. CD40 is required for the optimal induction of protective immunity to Mycobacterium avium. Immunology 2004; 111:323-7.
61. Harshan KV, Gangadharam PR. In vivo depletion of natural killer cell activity leads to enhanced multiplication of Mycobacterium avium complex in mice. Infect Immun 1991; 59:2818-21.
62. Saunders BM, Cheers C. Intranasal infection of beige mice with Mycobacterium avium complex: Role of neutrophils and natural killer cells. Infection and Immunity 1996; 64:4236-41.

63. Appelberg R, Castro AG, Gomes S, Pedrosa J, Silva MT. Susceptibility of beige mice to Mycobacterium avium: role of neutrophils. Infect Immun 1995; 63:3381-7.
64. Petrofsky M, Bermudez LE. Neutrophils from Mycobacterium avium-infected mice produce TNF-alpha, IL-12, and IL-1 beta and have a putative role in early host response. Clin Immunol 1999; 91:354-8.
65. Appelberg R. Neutrophils and intracellular pathogens: beyond phagocytosis and killing. Trends Microbiol 2007; 15:87-92.
66. Abadie V, Badell E, Douillard P, Ensergueix D, Leenen PJ, Tanguy M, et al. Neutrophils rapidly migrate via lymphatics after Mycobacterium bovis BCG intradermal vaccination and shuttle live bacilli to the draining lymph nodes. Blood 2005; 106:1843-50.
67. Martino A. Mycobacteria and innate cells: critical encounter for immunogenicity. J Biosci 2008; 33:137-44.
68. Tian T, Woodworth J, Sköld M, Behar SM. In vivo depletion of CD11c+ cells delays the CD4+ T cell response to Mycobacterium tuberculosis and exacerbates the outcome of infection. J Immunol 2005; 175:3268-72.
69. Flórido M, Cooper AM, Appelberg R. Immunological basis of the development of necrotic lesions following Mycobacterium avium infection. Immunology 2002; 106:590-601.
70. Bermudez LE, Petrofsky M. Host defense against Mycobacterium avium does not have an absolute requirement for major histocompatibility complex class I-restricted T cells. Infect Immun 1999; 67:3108-11.
71. Co DO, Hogan LH, Kim SI, Sandor M. Mycobacterial granulomas: keys to a long-lasting host-pathogen relationship. Clin Immunol 2004; 113:130-6.
72. Ramakrishnan L. Revisiting the role of the granuloma in tuberculosis. Nat Rev Immunol 2012; 12:352-66.
73. Guirado E, Schlesinger LS. Modeling the Mycobacterium tuberculosis Granuloma - the Critical Battlefield in Host Immunity and Disease. Front Immunol 2013; 4:98.
74. Ehlers S, Benini J, Held HD, Roeck C, Alber G, Uhlig S. Alphabeta T cell receptor-positive cells and interferon-gamma, but not inducible nitric oxide synthase, are critical for granuloma necrosis in a mouse model of mycobacteria-induced pulmonary immunopathology. J Exp Med 2001; 194:1847-59.
75. Flórido M, Appelberg R. Granuloma necrosis during Mycobacterium avium infection does not require tumor necrosis factor. Infect Immun 2004; 72:6139-41.
76. Ehlers S, Benini J, Kutsch S, Endres R, Rietschel ET, Pfeffer K. Fatal granuloma necrosis without exacerbated mycobacterial growth in tumor necrosis factor receptor p55 gene-deficient mice intravenously infected with Mycobacterium avium. Infect Immun 1999; 67:3571-9.
77. Borges M, Rosa GT, Appelberg R. The death-promoting molecule tumour necrosis factor-related apoptosis inducing ligand (TRAIL) is not required for the development of peripheral lymphopenia or granuloma necrosis during infection with virulent Mycobacterium avium. Clin Exp Immunol 2011; 164:407-16.
78. Kondo S, Sauder DN. Tumor necrosis factor (TNF) receptor type 1 (p55) is a main mediator for TNF-alpha-induced skin inflammation. Eur J Immunol 1997; 27:1713-8.
79. Flynn JL, Goldstein MM, Chan J, Triebold KJ, Pfeffer K, Lowenstein CJ, et al. Tumor necrosis factor-alpha is required in the protective immune response against Mycobacterium tuberculosis in mice. Immunity 1995; 2:561-72.
80. Wang S, El-Deiry WS. TRAIL and apoptosis induction by TNF-family death receptors. Oncogene 2003; 22:8628-33.
81. Falschlehner C, Schaefer U, Walczak H. Following TRAIL's path in the immune system. Immunology 2009; 127:145-54.
82. Flórido M, Appelberg R. Genetic control of immune-mediated necrosis of Mycobacterium avium granulomas. Immunology 2006; 118:122-30.

83. Actor JK, Breij E, Wetsel RA, Hoffmann H, Hunter RL, Jagannath C. A role for complement C5 in organism containment and granulomatous response during murine tuberculosis. Scand J Immunol 2001; 53:464-74.
84. Czermak BJ, Sarma V, Bless NM, Schmal H, Friedl HP, Ward PA. In vitro and in vivo dependency of chemokine generation on C5a and TNF-alpha. J Immunol 1999; 162:2321-5.
85. Via LE, Lin PL, Ray SM, Carrillo J, Allen SS, Eum SY, et al. Tuberculous granulomas are hypoxic in guinea pigs, rabbits, and nonhuman primates. Infect Immun 2008; 76:2333-40.
86. Benini J, Ehlers EM, Ehlers S. Different types of pulmonary granuloma necrosis in immunocompetent vs. TNFRp55-gene-deficient mice aerogenically infected with highly virulent Mycobacterium avium. J Pathol 1999; 189:127-37.
87. Aly S, Wagner K, Keller C, Malm S, Malzan A, Brandau S, et al. Oxygen status of lung granulomas in Mycobacterium tuberculosis-infected mice. J Pathol 2006; 210:298-305.
88. Harper J, Skerry C, Davis SL, Tasneen R, Weir M, Kramnik I, et al. Mouse model of necrotic tuberculosis granulomas develops hypoxic lesions. J Infect Dis 2012; 205:595-602.
89. Maltepe E, Saugstad OD. Oxygen in health and disease: regulation of oxygen homeostasis--clinical implications. Pediatr Res 2009; 65:261-8.
90. Scholz CC, Taylor CT. Targeting the HIF pathway in inflammation and immunity. Curr Opin Pharmacol 2013; 13:646-53.
91. Weidemann A, Johnson RS. Biology of HIF-1alpha. Cell Death Differ 2008; 15:621-7.
92. Palmer BF, Clegg DJ. Oxygen sensing and metabolic homeostasis. Mol Cell Endocrinol 2014.
93. Pugh CW, Ratcliffe PJ. Regulation of angiogenesis by hypoxia: role of the HIF system. Nat Med 2003; 9:677-84.
94. Haase VH. Regulation of erythropoiesis by hypoxia-inducible factors. Blood Rev 2013; 27:41-53.
95. Corzo CA, Condamine T, Lu L, Cotter MJ, Youn JI, Cheng P, et al. HIF-1α regulates function and differentiation of myeloid-derived suppressor cells in the tumor microenvironment. J Exp Med 2010; 207:2439-53.
96. Greijer AE, van der Wall E. The role of hypoxia inducible factor 1 (HIF-1) in hypoxia induced apoptosis. J Clin Pathol 2004; 57:1009-14.
97. Ke Q, Costa M. Hypoxia-inducible factor-1 (HIF-1). Mol Pharmacol 2006; 70:1469-80.
98. Shweiki D, Itin A, Soffer D, Keshet E. Vascular endothelial growth factor induced by hypoxia may mediate hypoxia-initiated angiogenesis. Nature 1992; 359:843-5.
99. Hayashi M, Sakata M, Takeda T, Yamamoto T, Okamoto Y, Sawada K, et al. Induction of glucose transporter 1 expression through hypoxia-inducible factor 1alpha under hypoxic conditions in trophoblast-derived cells. J Endocrinol 2004; 183:145-54.
100. Tacchini L, Bianchi L, Bernelli-Zazzera A, Cairo G. Transferrin receptor induction by hypoxia. HIF-1-mediated transcriptional activation and cell-specific post-transcriptional regulation. J Biol Chem 1999; 274:24142-6.
101. Carroll VA, Ashcroft M. Role of hypoxia-inducible factor (HIF)-1alpha versus HIF-2alpha in the regulation of HIF target genes in response to hypoxia, insulin-like growth factor-I, or loss of von Hippel-Lindau function: implications for targeting the HIF pathway. Cancer Res 2006; 66:6264-70.
102. Hu CJ, Wang LY, Chodosh LA, Keith B, Simon MC. Differential roles of hypoxia-inducible factor 1alpha (HIF-1alpha) and HIF-2alpha in hypoxic gene regulation. Mol Cell Biol 2003; 23:9361-74.
103. Greer SN, Metcalf JL, Wang Y, Ohh M. The updated biology of hypoxia-inducible factor. EMBO J 2012; 31:2448-60.
104. Elbarghati L, Murdoch C, Lewis CE. Effects of hypoxia on transcription factor expression in human monocytes and macrophages. Immunobiology 2008; 213:899-908.

105. Burke B, Tang N, Corke KP, Tazzyman D, Ameri K, Wells M, et al. Expression of HIF-1alpha by human macrophages: implications for the use of macrophages in hypoxia-regulated cancer gene therapy. J Pathol 2002; 196:204-12.
106. Strehl C, Fangradt M, Fearon U, Gaber T, Buttgereit F, Veale DJ. Hypoxia: how does the monocyte-macrophage system respond to changes in oxygen availability? J Leukoc Biol 2014; 95:233-41.
107. Kennedy A, Ng CT, Biniecka M, Saber T, Taylor C, O'Sullivan J, et al. Angiogenesis and blood vessel stability in inflammatory arthritis. Arthritis Rheum 2010; 62:711-21.
108. Lewis JS, Lee JA, Underwood JC, Harris AL, Lewis CE. Macrophage responses to hypoxia: relevance to disease mechanisms. J Leukoc Biol 1999; 66:889-900.
109. Cramer T, Yamanishi Y, Clausen BE, Förster I, Pawlinski R, Mackman N, et al. HIF-1alpha is essential for myeloid cell-mediated inflammation. Cell 2003; 112:645-57.
110. Anand RJ, Gribar SC, Li J, Kohler JW, Branca MF, Dubowski T, et al. Hypoxia causes an increase in phagocytosis by macrophages in a HIF-1alpha-dependent manner. J Leukoc Biol 2007; 82:1257-65.
111. Peyssonnaux C, Datta V, Cramer T, Doedens A, Theodorakis EA, Gallo RL, et al. HIF-1alpha expression regulates the bactericidal capacity of phagocytes. J Clin Invest 2005; 115:1806-15.
112. Thiel M, Caldwell CC, Kreth S, Kuboki S, Chen P, Smith P, et al. Targeted deletion of HIF-1alpha gene in T cells prevents their inhibition in hypoxic inflamed tissues and improves septic mice survival. PLoS One 2007; 2:e853.
113. Kojima H, Gu H, Nomura S, Caldwell CC, Kobata T, Carmeliet P, et al. Abnormal B lymphocyte development and autoimmunity in hypoxia-inducible factor 1alpha -deficient chimeric mice. Proc Natl Acad Sci U S A 2002; 99:2170-4.
114. Walmsley SR, Print C, Farahi N, Peyssonnaux C, Johnson RS, Cramer T, et al. Hypoxia-induced neutrophil survival is mediated by HIF-1alpha-dependent NF-kappaB activity. J Exp Med 2005; 201:105-15.
115. Jantsch J, Chakravortty D, Turza N, Prechtel AT, Buchholz B, Gerlach RG, et al. Hypoxia and hypoxia-inducible factor-1 alpha modulate lipopolysaccharide-induced dendritic cell activation and function. J Immunol 2008; 180:4697-705.
116. Köhler T, Reizis B, Johnson RS, Weighardt H, Förster I. Influence of hypoxia-inducible factor 1α on dendritic cell differentiation and migration. Eur J Immunol 2012; 42:1226-36.
117. Dang EV, Barbi J, Yang HY, Jinasena D, Yu H, Zheng Y, et al. Control of T(H)17/T(reg) balance by hypoxia-inducible factor 1. Cell 2011; 146:772-84.
118. Shi LZ, Wang R, Huang G, Vogel P, Neale G, Green DR, et al. HIF1alpha-dependent glycolytic pathway orchestrates a metabolic checkpoint for the differentiation of TH17 and Treg cells. J Exp Med 2011; 208:1367-76.
119. Isoe T, Makino Y, Mizumoto K, Sakagami H, Fujita Y, Honjo J, et al. High glucose activates HIF-1-mediated signal transduction in glomerular mesangial cells through a carbohydrate response element binding protein. Kidney Int 2010; 78:48-59.
120. Blouin CC, Pagé EL, Soucy GM, Richard DE. Hypoxic gene activation by lipopolysaccharide in macrophages: implication of hypoxia-inducible factor 1alpha. Blood 2004; 103:1124-30.
121. Zhou J, Schmid T, Brüne B. Tumor necrosis factor-alpha causes accumulation of a ubiquitinated form of hypoxia inducible factor-1alpha through a nuclear factor-kappaB-dependent pathway. Mol Biol Cell 2003; 14:2216-25.
122. Takeda N, O'Dea EL, Doedens A, Kim JW, Weidemann A, Stockmann C, et al. Differential activation and antagonistic function of HIF-{alpha} isoforms in macrophages are essential for NO homeostasis. Genes Dev 2010; 24:491-501.
123. van Uden P, Kenneth NS, Rocha S. Regulation of hypoxia-inducible factor-1alpha by NF-kappaB. Biochem J 2008; 412:477-84.

124. Kuhn A, Brachtendorf G, Kurth F, Sonntag M, Samulowitz U, Metze D, et al. Expression of endomucin, a novel endothelial sialomucin, in normal and diseased human skin. J Invest Dermatol 2002; 119:1388-93.
125. Gordon S, Lawson L, Rabinowitz S, Crocker PR, Morris L, Perry VH. Antigen markers of macrophage differentiation in murine tissues. Curr Top Microbiol Immunol 1992; 181:1-37.
126. Peyssonnaux C, Boutin AT, Zinkernagel AS, Datta V, Nizet V, Johnson RS. Critical role of HIF-1alpha in keratinocyte defense against bacterial infection. J Invest Dermatol 2008; 128:1964-8.
127. Pearl JE, Saunders B, Ehlers S, Orme IM, Cooper AM. Inflammation and lymphocyte activation during mycobacterial infection in the interferon-gamma-deficient mouse. Cell Immunol 2001; 211:43-50.
128. Orme I. Cellular and genetic mechanisms underlying susceptibility of animal models to tuberculosis infection. Novartis Found Symp 1998; 217:112-7; discussion 7-9.
129. Aly S, Laskay T, Mages J, Malzan A, Lang R, Ehlers S. Interferon-gamma-dependent mechanisms of mycobacteria-induced pulmonary immunopathology: the role of angiostasis and CXCR3-targeted chemokines for granuloma necrosis. J Pathol 2007; 212:295-305.
130. Riboldi E, Porta C, Morlacchi S, Viola A, Mantovani A, Sica A. Hypoxia-mediated regulation of macrophage functions in pathophysiology. Int Immunol 2013; 25:67-75.
131. Clay H, Volkman HE, Ramakrishnan L. Tumor necrosis factor signaling mediates resistance to mycobacteria by inhibiting bacterial growth and macrophage death. Immunity 2008; 29:283-94.